

Mechanical and Structural Properties of Highly Loaded Carbon Nanotubes/Polyamide 6 Composites

by

Normarieli M. Passalacqua Alvarado

A thesis submitted in partial fulfillment of the requirements for the degree of

MASTER OF SCIENCE

in

MATERIALS SCIENCE AND ENGINEERING

UNIVERSITY OF PUERTO RICO

MAYAGUEZ CAMPUS

May 2019

Approved by:

Carlos Marín Martín, PhD
Chairperson, Graduate Committee

Date

O. Marcelo Suárez, PhD
Member, Graduate Committee

Date

Agnes M. Padovani, PhD
Member, Graduate Committee

Date

Aidsa Santiago Román, PhD
Director of Eng. Sci. & Mat. Dept.

Date

Carla López del Puerto, PhD
Representative of Graduate Studies

Date

ABSTRACT

Recently, carbon-fiber composite materials have been attractive to many industries and agencies such as automotive, aerospace, sport equipment manufacturing, Department of Defense, and Department of Energy. These materials show improved mechanical properties and can be lighter than steel and many other alloys. Carbon nanotubes are structures that present unique chemical and mechanical properties, such as sp^2 hybridization and an elastic modulus of about 1 TPa, which make them a suitable prospective to enhance the properties provided by the carbon fibers. Reported studies have showed that carbon nanotubes can be used as fillers in different polymeric matrices such as epoxy, polyether ether ketone, polycarbonate, polyamides, and others. However, obtaining a good dispersion of carbon nanotubes in the matrix is quite challenging, because their electrostatics forces make them to agglomerate. In order to get a better interaction between the carbon nanotubes and the polymer matrix, many researchers have tried to functionalize the carbon nanotubes surfaces. However, functionalization of the carbon nanotube surfaces might end in reduction of their chemical and mechanical properties. In this study, non-functionalized carbon nanotubes/polyamide 6 composites were fabricated using an innovative method where no solvent is needed. Concentrations of carbon nanotubes (40-65 wt%), higher than ever reported were used to create the composites. Temperatures higher than the melting point of the polymer and pressure was required to fabricate the composites. Pressure levels and processing temperature were found to have a strong effect on the final composites' structure. For this reason, two different temperatures (280-300 °C), and two different pressures (5 and 10 MPa) were studied. Higher polyamide 6 degradation was found for polymer samples processed under air atmosphere at 300 °C, than for the samples processed under nitrogen atmosphere. Larger number of defects was found for the composites processed at 5 MPa of pressure compared to the ones processed applying a pressure of 10 MPa. An improvement in the polyamide 6 mechanical properties, such as the hardness and the elastic modulus, was found for the carbon nanotubes loaded composites.

RESUMEN

Los materiales a base de carbono (por ejemplo, fibras de carbono) han captado la atención de varias industrias y agencias tales como la automotriz, aeroespacial, compañías donde se fabrica equipo deportivo, Departamento de Defensa y Departamento de Energía. Estos materiales pueden llegar a presentar mejores propiedades mecánicas y a la vez ser más livianos que el acero y muchas otras aleaciones. Los nanotubos de carbono en especial presentan propiedades químicas y mecánicas únicas, por ejemplo, tienen una hibridación sp^2 y un módulo de elasticidad de aproximadamente 1 TPa, lo que los convierte en buen prospecto para reemplazar las fibras de carbono. Estudios reportados recientemente han demostrado cómo los nanotubos de carbono se pueden utilizar como rellenos en compuestos con diferentes matrices poliméricas como el epoxi, poliéter éter cetona, policarbonato, poliamidas y otros. Sin embargo, lograr una buena dispersión de los nanotubos de carbono en la matriz polimérica puede resultar bastante difícil, porque las fuerzas electrostáticas en la superficie de los nanotubos hacen que se estos se aglomeren. Para lograr un buen enlace entre los nanotubos de carbono y la matriz polimérica, muchos investigadores han intentado funcionalizar las superficies de los nanotubos. Sin embargo, la funcionalización de la superficie de los nanotubos de carbono podría resultar en una restricción o disminución de sus propiedades químicas y mecánicas. En este estudio, se fabricaron compuestos de nanotubos de carbono (no funcionalizados) / poliamida 6 utilizando un método innovador donde no se necesita solvente. En la fabricación de los compuestos, se utilizaron concentraciones de nanotubos de carbono (40-65% por peso) más altas que las que han sido reportadas anteriormente. Se encontró que el procesar los compuestos a una temperatura sobre el punto de fusión del polímero y que el aplicar presión durante este paso tiene un efecto en su estructura final. Por esta razón, se utilizaron dos temperaturas (280-300 °C) y dos presiones (5 y 10 MPa) distintas durante el procesamiento de los compuestos. Se encontró que ocurre mayor degradación de poliamida 6 cuando las muestras son procesadas en atmósfera de aire a 300 °C que para las muestras procesadas en una atmósfera de nitrógeno. Además, se encontró un mayor número de defectos para aquellos compuestos a los cuales se le aplicó una presión de 5 MPa, en comparación con los que se procesaron aplicando una presión de 10 MPa. Se encontró una mejora en las propiedades mecánicas, tales como la dureza y el módulo de elasticidad, de los compuestos al agregar los nanotubos de carbono.

Copyright © by
Normarieli Passalacqua-Alvarado
2019

ACKNOWLEDGEMENTS

I would like to acknowledge the Office of Naval Research (ONR) for supporting this project. In addition, I want to thank the Transformational Initiative for Graduate Education and Research (TIGER) program (#P031M140035), for supporting my academic and professional development. All the composites were fabricated in facilities of the University of Puerto Rico at Mayagüez. The characterization and the mechanical analysis were done in the Material Science Research and Engineering Center (DMR-1720415) from the University of Wisconsin-Madison College of Engineering. Finally, this study was completed thanks to the principal investigator, Dr. Carlos Marín and to the rest of my graduate committee, Dr. Oscar Marcelo, and Dra. Agnes Padovani.

TABLE OF CONTENTS

List of Figures	viii
List of Tables	x
Chapter 1. Introduction	1
1.1. <i>Properties and Applications</i>	1
1.2. <i>Literature Review</i>	2
1.3. <i>Justification</i>	7
1.4. <i>Objectives</i>	9
Chapter 2. Theoretical Background	10
2.1. <i>Polymers</i>	10
2.1.1 Polymers with Linear-Unbranched Chains	10
2.1.2 Thermoplastic Polymers	11
2.1.3 Deformation of Polyamides	15
2.2. <i>Carbon Nanotubes</i>	16
2.2.1 Atomic Structure of Carbon Nanotubes	16
2.2.2 Methods to Synthesize Carbon Nanotubes	20
2.2.3 Mechanical Properties of Carbon Nanotubes	22
2.2.4 Non-Covalent Functionalization	23
2.3. <i>Composites Materials</i>	23
2.3.1 Polymer-Matrix Composites	24
2.3.2 Short-Fiber (Carbon Nanotubes) Reinforcement	24
2.3.3 Composite's Behavior at the Interface	25
2.3.4 Interactions at the Composite's Interface: Mechanical and Physical Bonding	27
2.3.5 Mechanical Properties	28
2.3.6 Melt Pressing Method	29
Chapter 3. Methodology	30
3.1. <i>Materials</i>	30
3.3. <i>Sample Processing</i>	32
3.4. <i>Composite Analysis</i>	35
Chapter 4. Carbon Nanotube/Polyamide 6 Structural Characterization	38
4.1. <i>Microscopy</i>	38
4.2. <i>Thermal Gravimetical Analysis</i>	45

Chapter 5. Mechanical Properties of Carbon Nanotubes/Polyamide 6 Composites	52
5.1. <i>Vickers Hardness</i>	52
5.2. <i>Elastic Modulus of Carbon Nanotubes/Polyamide 6 Composites</i>	55
Chapter 6. Conclusions and Future Work	59
References	62

LIST OF FIGURES

Figure 2. 1. Structure of linear polymers.	11
Figure 2. 2. Changes of the semi-crystalline polymers in response to the temperature.	13
Figure 2. 3. Behavior of semi-crystalline polymers.	13
Figure 2. 4. General mechanical behavior of thermoplastics.	14
Figure 2. 5. Structure of (a) SWCNTs and (b) MWCNTs.	16
Figure 2. 6. Chirality of CNTs.	17
Figure 2. 7. Lennard- Jones potential diagram for two interacting carbon atoms.	19
Figure 2. 8. The Lennard-Jones force in carbon nanotubes.	20
Figure 2. 9. a) Aligned fiber and b) randomly organized fibers in a matrix.	25
Figure 2. 10. Relation between the gripping stress (σ_r) and the interfacial shear stress (τ_i).	28
Figure 2. 11. (A) Good mechanical bond (B) poor wetting between the matrix in the liquid state and the filler surface.	28
Figure 3. 1. General CNTs/polymer composites fabrication method.	31
Figure 3. 2. Real representation of the CNTs/polymer composites' fabrication.	31
Figure 3. 3. First hot press used to fabricate CNTs/PEEK composites.	33
Figure 3. 4. First and second hot press machine used for the composites' manufacturing.	34
Figure 3. 5. The two heat treatments used to fabricate CNT/PA6 composites, at 280 °C and at 300 °C.	35
Figure 3. 6. Vickers Hardness test and micro-indentation.	36
Figure 3. 7. Dynamic Mechanical Analysis.	37
Figure 4. 1. Preprocessed carbon nanotubes.	38
Figure 4. 2. MWCNT/PA6 composites' cross-sectional area after fracture without polishing.	39
Figure 4. 3. MWCNT/PA6 composites at high magnification.	40
Figure 4. 4. SWCNT/PA6 composites' cross-sectional area after fracture without polishing	42
Figure 4. 5. SWCNT/PA6 composites at high magnification.	42
Figure 4. 6. 55 wt% MWCNTs/PA6 composites processed with an applied pressure of 5 MPa.	44
Figure 4. 7. 55 wt% MWCNT/PA6 composites processed with an applied pressure of 10 MPa.	44
Figure 4. 8. 55 wt% SWCNT/PA6 composites processed with an applied pressure of 5 MPa.	45
Figure 4. 9. Thermal degradation under nitrogen and air atmosphere of neat polyamide 6 a) at 280 °C and at b) at 300 °C.	46

Figure 4. 10. Polyamide 6 proposed decomposition mechanism by a) Levichik et al. and b) by Zhao et al.	48
Figure 4. 11. Thermal degradation in nitrogen and air atmosphere of SWNT/PA6 composites a) at 280°C and at b) at 300°C.	50
Figure 5. 1. Hardness test for MWCNT/PA6 composites with different CNT concentrations and processed with a 0.30 mm thick spacer, at 280 °C with an applied pressure of 5 MPa.	53
Figure 5. 2. Hardness test for MWCNT/PA6 composites with different CNT concentrations and processed with a 0.30 mm thick spacer, at 280 °C with an applied pressure of 10 MPa.	54
Figure 5. 3. Hardness test for 55 WT% CNTs/PA6 composites processed with a 0.30 mm thick spacer, at 280 °C, and with an applied pressure of 5 MPa.	55
Figure 5. 4. Stress versus strain curve for CNT/PA6 composites.	56
Figure 5. 5. Values of elastic modulus for MWNT/PA6 composites at different CNT concentrations.	57

LIST OF TABLES

Table 1. 1. Summary of the most relevant results
--

8

CHAPTER 1. INTRODUCTION

“Global Composites Market is Projected to Reach \$42 Billion by 2022”. This was the title of an article published in the Research and Markets magazine in June 22, 2018. This is including both glass and carbon fibers and their great demand for civil engineering, aerospace & defense, automotive industry, and sport equipment manufacturing industries. The reason why composites have such a high demand is their light weight, and fuel economy. [1] According to the Machine Design magazine, from those \$42 billion up to \$31 billion come from the carbon fiber composite market. [2] In addition, it was reported in the Composites Manufacturing magazine that the Federal Aviation Administration approved the design for Boeing’s folding Carbon Fiber Reinforced Polymer (CFRP) wingtips that will be incorporated in two 777X aircraft variants, the 777-8 and 777-9, models that will go out to market on December 2019. [3] The composite industry has been growing globally, BMW is also currently using composite technologies for its future models. [3] These examples only consider CFRP. In contrast, composites containing stronger materials than carbon fibers such as carbon nanotubes are not reaching the forecasted market. The reason why carbon nanotubes reinforced polymers technology is not currently marketed is because of the obstacles that these materials are facing in the manufacturing process. This study aims to remove some of those obstacles and focus on carbon nanotube reinforced polyamide 6 as a contribution to make them industrially available.

1.1. PROPERTIES AND APPLICATIONS

Carbon nanotubes (CNTs) have been widely studied because of their remarkable properties. Their exceptional chemical, electrical, thermal, and mechanical properties make them a practical material for applications, such as aerospace engineering and automotive manufacturing. There are different types of CNTs: single-walled carbon nanotubes (SWCNTs), which are composed of a single wound graphene sheet, and multi-walled carbon nanotubes (MWCNTs), which are composed of two or more wound graphene sheets. Due to their sp^2 hybridization or double carbon-carbon bond, they have a bond energy of ~ 628 kJ/mol, which is larger than single carbon-carbon bonds. In addition, they have electrostatic forces such as π - π interactions (van der Waals forces), which create an attraction force to other CNTs or compounds with similar electronic configuration. [4] Furthermore, it was found that CNTs can have an elastic modulus above 1000

GPa along their length and a low density between 1.3 to 1.4 g/cm³. This means that they can be stronger, but also lighter than other types of materials such as steel, which has an elastic modulus of approximately 200 GPa. [5], [6]

CNTs are used to reinforce polymers such as polyamide 6 (PA6) to benefit from load transfer and improve mechanical properties. PA6 is a thermoplastic compound characterized for having a high elastic modulus of 3.3 GPa. They also have other distinctive mechanical properties such as high tensile and impact strength. The use of this polymer is ideal because it is a non-toxic compound. Semi-crystalline pure PA6 is mostly used as aircraft tire reinforcement, and it is also used in automotive components. PA6 has relatively moderate heat resistance and can be combined with other materials without significant degradation. [7]–[9]

A hot-pressing method is used to fabricate the CNTs/polymer composites. This method is considered environmentally friendly since no hazardous solvents are used; and uses a layered initial configuration of compounds to produce composites with a homogeneous CNT dispersion. In addition, it does not need expensive techniques or equipment to purify the CNTs to obtain the desired product. By using the layered starting configuration, this technique intends to avoid lack of homogeneity due to interactions between the CNTs and the matrix. The objective is to avoid fissures or porosity in the final samples. These fissures or pores represent concentrated stress that can lead to material failure. For this reason, it is important to minimize the porosity and, hence, improve the elastic modulus of the final composite. Once this is accomplished, stronger materials will be obtained. The purpose of this study is to evaluate how factors such as the composition of the CNTs in the matrix, the temperature and the pressure applied at the maximum point during the heat treatment, and the type of CNTs might have an effect in the composite's elastic modulus.

1.2. LITERATURE REVIEW

CNT/polymer composites have been widely used for aerospace and automobile industries due to their remarkable thermal, electrical and mechanical properties. [10] However, they also have been recently implemented in biomedical applications, namely prosthetic devices. These composites can easily transfer heat and show unique mechanical properties, such as high elastic

modulus, unlike the materials used in currently available prostheses. Materials that store heat might create skin maceration, causing bacterial invasion. Researchers have attempted to fabricate CNT/epoxy-based composites for this purpose. [11] Since a successful interaction between the CNTs and the polymer or matrix is very difficult, many researchers have tried to modify or functionalize the CNT's surface to produce a better bond [11], [12], even though it is an expensive and rigorous process. Several of these studies regarding the modification of CNTs will be discussed in detail. [11]–[14]

Mahmood et al., have reported pristine and functionalized MWCNT/PA6 composites. [12] They prepared amine-functionalized CNTs using a reflux treatment. In order to successfully complete the modification, the chemical treatment was completed with HCl, HNO₃, and H₂SO₄ (all of them are strong acids). The resulting product was nanocomposites with pure and amine-functionalized MWCNTs at 0.5 wt%. [12] Arun and Kanagaraj, have also functionalized the MWCNT surface to make MWCNTs/epoxy-based sandwich composites in order to improve their thermal and mechanical properties. [11] In their study, the composites were made at 0.1, 0.2, 0.3, 0.4, and 0.5 wt% of MWCNTs. After chemically treating the MWCNTs by adding C-O, C=C, C=O, and O-H bonds, and synthesizing the epoxy, Arun and Kanagaraj, dissolved each of them separately, the epoxy and MWCNTs, in acetone. Then, both solutions were mixed, and the acetone was removed through vacuum drying. The final epoxy-MWCNTs solution was then mixed with a hardener and processed to produce the sandwich composites. [11] In contrast to the studies previously discussed, in the present study, the CNTs will not be functionalized before the composite fabrication. This study, however, employs an alternate method to obtain CNT/polymer-based sandwich composites without altering or modifying any of the starting materials, in order to achieve a low-cost and environmentally friendly technique. It is also of interest to manufacture composites at a larger scale, in the order of millimeters, since the materials properties might vary depending on the order of magnitude. While, Mahmood et. al. and Arun and Kanagaraj, utilized an organic acid as a medium this study implemented a solid-state method, not requiring any of organic or inorganic solvent. [11], [12]

In the end, Mahmood et. al., synthesized the composites as thin films using a hot press at 235°C and 200 bar (20 MPa). [12] Careful attention must be paid to the pressure applied to the composites, because permanent deformation in the CNTs can occur. In general, CNTs are

characterized for being flexible, returning to their original shape after being bended or twisted. In order to perform the CNTs/polymer composites, it is necessary for the polymer to melt during the heating process. If high pressure is applied, when the polymer solidifies, it can permanently deform the CNTs, hindering their ability to return to their original shape. For this reason, the present study used pressures below 20 MPa. On the other hand, S. Arun and S. Kanagaraj, have carried out the composites fabrication steps near to room temperature, and atmospheric pressure. [11] Preliminary results of the present study showed that pressure is necessary to minimize the porosity in the composites. Therefore, pressure is considered an important factor.

Transmission electron microscopes (TEM) and scanning electron microscopes (SEM) are generally used to characterize the morphology of the composites. [11], [12] Mahmood et al. have confirmed crystallographic defects in the CNTs after being functionalized. [12] CNT functionalization involves an increase in their surface area. [15] This might explain the defects observed in the CNTs after being functionalized. From SEM micrographs, they have also reported a better dispersion of CNTs appearance in the PA6/amine-functionalized CNTs composites than in those composites with non-functionalized CNTs. [12] Arun and Kanagaraj reported diameters of 15 and 40 μm for the voids found in the samples at 0.4 and 0.5 wt % of MWCNTs, respectively [11]. In contrast to these studies, the goal of this current research is to fabricate sandwich composites at higher concentrations of CNTs. Thus, reducing the porosity and achieving a homogeneous dispersion of CNTs in the matrix without the necessity of functionalizing the CNT's surface.

Arun and Kanagaraj have also reported for the CNT/epoxy samples with a composition of MWCNTs 0.3 wt%, a compressive modulus of approximately 3.45 GPa with a reinforcement increased by 20.2%, compared with pure epoxy. The researchers have confirmed stress transfer from the epoxy to MWCNTs after comparing the Raman spectra of the composites before and after the compressive test. They found a shift in the G-band, which is consistent with an effective stress transfer, resulting in enhanced mechanical properties. According to the researchers, the composites with a MWCNT content more than 0.3 wt% showed poorer mechanical properties than those with higher compositions. This is due to an increase in viscosity, specific surface area, and voids after being modified. Hence, higher MWCNTs compositions compromise the wetting process between the polymer and the MWCNTs. [11]

Furthermore, Palardy et. al. studied the morphology and the mechanical properties of MWCNT/polyamide 12 (nylon 12) fiber composites. The difference between the polyamide 6 (PA6) and polyamide 12 (PA12) is the additional six CH_2 chains between the amide group (R-NH-R') and the carbonyl group (C=O). Thus, the PA12 chain is longer than the PA6. The researchers worked with compositions of 0, 1.0, 2.0, and 5.0 wt% of MWCNTs, and after fabricating the MWCNT/PA12 pellets using a twin-screw industrial extruder at 200°C , they were again extruded, in this case, with a *Rosand* capillary rheometer to produce the fiber structure. Palardy et. al. described the microstructure of the MWCNT/PA12 fibers with small agglomeration of CNTs in some parts, but in general, their distribution was mostly uniform. The researchers have reported the stress-strain curves for samples post drawn at 100°C , 300% elongation; 120°C , 300% elongation; and 140°C , 500% elongation. They used these temperatures because they are above the composite glass transition temperature (T_g), but below its melting temperature. According to them, the samples with higher MWCNT compositions (5.0 wt%) have exhibited an elastic modulus of 3.8 GPa (with 500% elongation and at 140°C). [14]

Moreover, Pande et al. analyzed the ability of CNTs to enhance the electrical and mechanical properties of the polymer by load transfer. The researchers used non-functionalized, or as-synthesized-MWCNTs (a-MWCNTs) and functionalized MWCNTs (f-MWCNTs). The f-MWCNTs were functionalized using nitric acid (HNO_3). Afterwards, the authors fabricated the composites using the solvent casting technique. After having the a-MWCNTs and the f-MWCNTs, each of them was dispersed in tetrahydrofuran (THF) for 2 hours until homogeneous mixtures with the ensuring concentrations were obtained from 0.1wt% to 23 wt% of a-MWCNTs, and from 0.1wt% to 5 wt% of f-MWCNTs in the matrix. To form a homogeneous dispersion of MWCNTs in polycarbonate (PC), the researchers magnetically stirred the mixtures for 24 hours. The composites films were cast from the homogeneous solution by pouring the solution into a Teflon spray coated Petri dish and allowing the solvent to evaporate during three to five days, followed by drying in an oven. Pande and colleagues also wanted to study the effect on applying both contact pressure ($\sim 10\text{ kg/cm}^2$) to some samples and full pressure ($\sim 10\text{ kg/cm}^2$) to others. In both cases, the pressures were applied during a heat treatment at 170°C . In order to achieve a desirable thickness, they placed the composite samples in a specially fabricated die (60 mm x 20 mm x 2 mm). [13] A similar procedure was performed by Jindal et al. who wanted to test the mechanical properties of the MWCNT/PC composites employing nano indentation. However, in

this study, only non-functionalized MWCNTs were studied with the following compositions: 0.5, 0.75, 2.0, 5.0, and 10 wt% in pure PC. In contrast to Pande et al., Jindal and colleagues ultrasonically disturbed the MWCNTs and PC powder in chloroform instead of THF in order to achieve a homogeneously dispersion of the MWCNTs in PC. [16] As was mentioned before, in the current study the composite fabrication will be performed without dissolving the CNTs in any kind of reagent and without the necessity to modify the CNTs surface.

Pande and collaborators obtained composites with a thickness of about 1.8 to 2.0 mm. After testing the mechanical properties of the composites, they reported an elastic modulus of 1.6 GPa for the one containing 20 wt% of a-MWCNTs. For those composites, the researchers reported a 43% increase from the pure PC fabricated by following the same process to fabricate the composites. [13] In the case of Jindal and colleagues, an elastic modulus and a hardness value of 6.99 GPa and 382.77 MPa was respectively obtained for 10 wt% MWCNT/PC composites. [16] According to Pande et al., the composite's ductility decreases with an increasing of the CNTs concentration, all the while the composite becomes more brittle. Pande et al. reported lower elastic modulus values for f-MWCNT/PC composites in comparison with the composites containing a-MWCNTs. They mentioned that this could be attribute to the CNT length. Shortened f-MWCNTs are less effective than longer a-MWCNTs in restricting mobility of polymer chains. [13] In addition, Jindal and colleagues found higher elastic modulus and hardness at greater CNTs concentrations in PC for those composites containing non-functionalized MWCNTs. According to the researchers this tendency could be due to the stronger short-range interactions between PC molecules mediated by MWCNTs and lasts up to some critical concentration of MWCNTs. [16] To prove this issue, using Molecular Dynamics (MD), Sharma et al. simulated a MWCNT/PC system under the same conditions of Jindal and collaborators. They reported higher elastic modulus when the MWCNT percentage increases up to 10 wt %. Moreover, they found a slight increase of shear modulus with an increase in the amount of CNTs. They reached the conclusion that composites with around 2 wt% of MWCNTs could be suitable to enhance both static and dynamic properties. [17]

1.3. JUSTIFICATION

Since carbon nanotubes are materials with extreme aspect ratio at the nano scale, making homogeneous polymer matrix composites using CNTs as fillers is challenging. Van der Waals forces cause agglomeration between each other making hard to achieve a homogeneous dispersion in the matrix. Many researchers have tried to overcome these challenges by using different techniques, fabrication methods, and surface treatments in the CNTs as have previously described. In this study, this type of composites is fabricated by employing a simple approach. The investigation that is presented here arises from previous studies conducted by the researcher group for fabrication of carbon nanotubes/poly (ether ether ketone), composites using the same method, which will be discussed in the next chapters. Those studies emerge after the findings reported by Bacsa et al. [18] who studied the dispersion of CNTs in a thermoplastic polymer, PEEK, through a thermal annealing. Basca and collaborators produced PEEK films by placing droplets of the polymer in powder form, dispersed in acetone, on a glass slide and letting them cure at 380 °C for 10 minutes in argon atmosphere. Subsequently, the researchers deposited the CNTs, which were previously sonicated and dispersed in acetone, on the PEEK film. They performed an annealing to the samples at 380 °C, which is above to the melting temperature of the polymer (343 °C). According to Basca et al., the polymer chains effectively diffuse around the CNTs surface at higher temperatures. The researchers suggest that this diffusion at high temperatures allows a better dispersion of the CNTs, because their thermal diffusion also increase with the temperature and favors the tube separation. The researchers also found a better dispersion for the SWCNTs than for MWCNTs. [18] It was our interest to indagate more in this topic and study the behavior of CNTs in presence of other thermoplastic polymers such as polyamide 6.

In addition, experiments have been conducted to study the mechanical properties of CNT/polymer composites but using relatively lower concentrations of CNT (less than 25 wt%) in the matrix. Table 1. 1 presents a summary of some of the more recent findings involving CNT/polymer composites which were discussed in detail in the previous section. Many of these studies present different methods or treatments in the CNTs surface involving organic or inorganic solvents to homogeneously disperse the tubes in the polymeric matrix. However, this study employed an innovative method where no solvent was needed. Concentrations higher than 40

wt% and pressures below 15 MPa are used in order to achieve a homogeneous dispersion of the CNTs in the matrix. This was accomplished to minimize the composite porosity and therefore enhance their elastic modulus.

Table 1. 1. Summary of the most relevant results

Author	Material	Fabrication Method	Conditions	Results
Arun and Kanagaraj [11]	MWNT/epoxy (films)	Hand lay-up technique	0.3 wt% At room temperature and atmospheric pressure	E: 3.45 GPa
Mahmood et al. [12]	p-MWCNT/PA6 n- MWCNT/PA6	Using a hot press	0.5 wt% At 235 °C and at 20 MPa	Low porosity
Palardy et al. [14]	MWNT/PA12 (fibers)	Extrusion with a Rosand capillary rheometer	0.5 wt% At 200 °C	E: 3.8 GPa
Pande et al. [13]	MWNT/PC (films)	Solvent casting technique	20 wt%	t: 1.8 mm to 2.0 mm E: 1.6 GPa
Jindal et al. [16]	MWNT/PC (films)	Solvent casting technique	10 wt%	E: 6.99 GPa H: 382.77 MPa Stress transfer confirmation
Morishita et al. [19]	MWNT/PA6/PPS/EDMA MWCNT/PA6/PPS/GOPTS	Melt-blend Twin-screw	1.75 wt%MWCNT At 200 °C Screw rotation rate 200 rpm	E': 3.22 GPa at 30 °C 1.08 GPa at 100 °C

E: elastic modulus; E': storage modulus t: thickness; H: Hardness

1.4. OBJECTIVES

The general objective of this research is to obtain a better understanding of the CNT behavior in a polymeric matrix to apply them as load bearing, impact sustaining, non-metallic structures in future applications such as aerospace and automotive industry.

The specific objectives of this research are:

- Prepare SWCNT/PA6 and MWCNT/PA6 sandwich type composites at different concentrations (wt%) of CNTs in the polymeric matrix.
- Characterize the CNT dispersion in the polymeric matrix.
- Determine the polymer degradation at two different temperatures during the heating process.
- Study the effect of the following factors in the composite's hardness: CNT concentrations in the matrix, CNT type (SWCNT or MWCNT), and applied pressure during the heating process.
- Determine the CNT/PA6 composite's elastic modulus and hardness.

CHAPTER 2. THEORETICAL BACKGROUND

In order to understand how a composite material behaves, it is important to also study and comprehend the nature of their components. In this chapter, concepts related to polymer, carbon nanotubes and composites materials will be discussed.

2.1. POLYMERS

A polymer consists of a chain of many repeated molecule units. The prefix “poly” means many, and the suffix “mer” means unit. These single units are called monomers and they are the principal components of the plastics materials. One of the many applications that polymers have is that they act as a matrix (solvent) in composites. Some polymers can be lightweight, corrosion resistance, and can be relatively inexpensive. [20] [21]

2.1.1 Polymers with Linear-Unbranched Chains

Polymers can be classified based on their molecular structure. Linear polymers are made of unit chains that resemble spaghetti structures (see Figure 2. 1), they can be branched or unbranched. Nevertheless, here will only discuss linear-unbranched polymers such as polyamide 6. In this type of polymer, each repeated unit is connected to another by strong covalent bonds. In other types of polymers, these connections between units could be made by weaker forces such as van der Waals forces. When these polymers are heated, they will increase the random movement of their monomers. This movement will try to overcome the secondary forces that are between the chains. After all forces are overcome, the units will freely move around and the polymer melts. This explains the thermoplastic nature of polymers. [22]

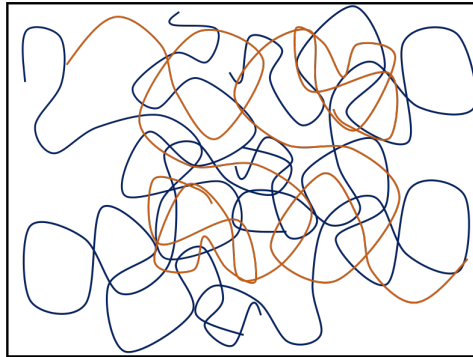


Figure 2. 1. Structure of linear polymers.

2.1.2 Thermoplastic Polymers

There is another way to classify polymers and this is related to their behavior under relatively high temperatures. Polymers could be thermosets or thermoplastics, in contrast to the thermoplastics, a thermoset polymer can only melt during the first-time heating process. When this type of polymer is heated for the first time, its structure will change from a one-dimensional to a three-dimensional bond network. [22] After the initial heating, a thermoset polymer is “cured”, and if is applied some temperature again, it will degrade instead of melting. This behavior does not occur in thermoplastic polymers. Thermoplastics could be heated and cooled more than once and will be able to conserve their properties. [21]

Thermoplastics usually are linear molecules. [21] In a single polymer chain, the monomers of this type of polymers are attached by strong covalent bonds. However, the type of bonds that can be found between the chains of thermoplastics are weaker forces such as van der Waals. These secondary bonds can be temporarily suspended when heat is applied. Polymers under this classification can be re-heated more than once without losing any of their properties. [22] In general, thermoplastics can have branched or un-branched linear chains. Their linear chains get tangled. Nevertheless, with the application of some tensile stress, these linear chains can untangle. Thermoplastics can have an amorphous or a semi-crystalline structure (i.e., polyamide 6). The emphasis of this section is discussing the behavior of thermoplastics since polyamide 6 is categorized as one.

a. Crystallinity in thermoplastics

Crystallinity can affect in certain way some properties of different materials. Some thermoplastic polymers are able to have both amorphous and crystalline regions. Crystalline regions will affect some properties of the polymers as well, including their mechanical properties. Crystal growth can result from temperature changes during the material processing or after applied certain stress. When a crystalline or partial crystalline polymer is experimenting some deformation, their chains will be forced to untangle, and they will start to align in a linear fashion. This activity will lead the crystallization in the material. During this process, the polymer chains could have a preferred orientation. This is useful to fabricate polymer fibers that could have better mechanical properties than many metals or ceramic materials (i.e., nylon fibers). In fact, this texture strengthening played a key role in the discovery of nylon fibers. [20] Having complex functionals groups attached will make harder the crystallization process in a thermoplastic. In addition, branched polymers usually present low crystallization. It is important to mention that the rearrangement of the polymer chains into a more orderly and packed structure might cause an increase in the material's density.

b. Temperature effect on thermoplastic polymers

The covalent bonds that unite the monomers in a thermoplastic can be destroyed under very high temperatures. As a consequence of this, the polymer may burn or char. In thermoplastic polymers, the decomposition occurs in the liquid state. Usually, thermoplastics do not have a specific melting temperature (T_M). Melting in thermoplastics can occur over a range of temperatures. For nylon-6,6, melting can occur between 220-260°C. For this reason, nylon could be processed between 260-327°C. During or above the T_M , the secondary bonds between the polymer chains become weaker. At this point, the polymer chains can slide from one to another if a force (i.e., pressure) is applied to it. Thus, the polymer flows with practically no elastic strain. The polymer sometimes presents a rubbery behavior when it is below of its T_M . Both, elastic and plastic deformation can occur, when a certain load is applied. After removing that applied load, the elastic deformation will be removed as well. At this point, the polymer might be permanently deformed, because of the movement of their chains. [20]

Temperature changes can also affect the thermoplastic's properties. Once they cooled below T_M , they can be amorphous or crystalline (see Figure 2. 2). Polymers that completely crystallize will not show a glass transition temperature (T_g). However, polymers that partially crystallize have amorphous regions that do have a glass transition state (see Figure 2. 3). Furthermore, linear amorphous polymers tend to be hard, brittle, and have a glassy behavior below T_g (see Figure 2. 3). Some properties such as density and elastic modulus might change at a different rate if the polymer cools below the T_g (see Figure 2. 3). [20]

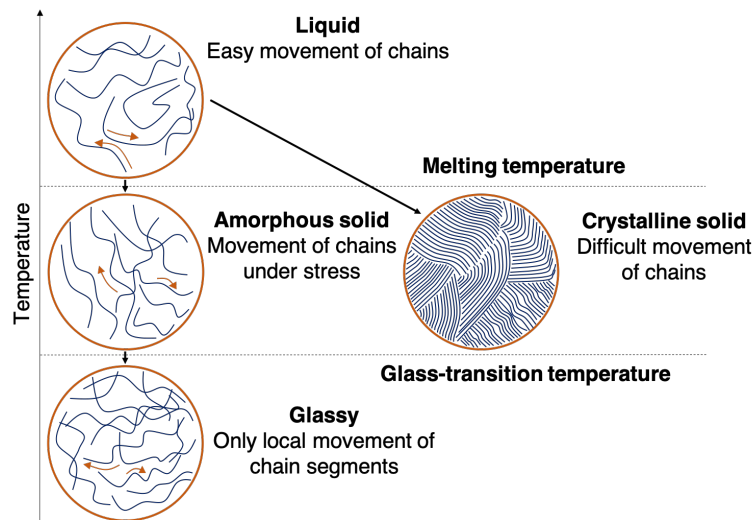


Figure 2. 2. Changes of the semi-crystalline polymers in response to the temperature.

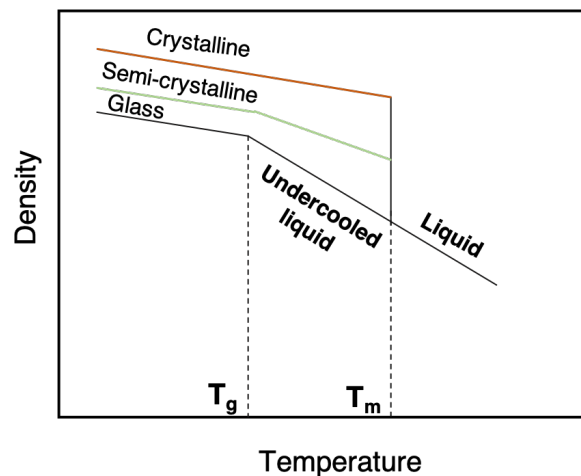


Figure 2. 3. Behavior of semi-crystalline polymers.

c. Mechanical properties of thermoplastic polymers

Thermoplastics usually show a non-Newtonian and viscoelastic behavior. This means that there is not a linear relationship in most of the parts on the stress-strain curve. On the other hand, a material shows viscoelastic behavior when both elastic and plastic deformations occur after applying an external force. The mechanical properties of a polymer are related to the movement of their chains under a certain applied force (load). In polymers, their deformation depends on the time and the rate at which the load is applied. In Figure 2. 4 is observed the stress-strain curve of nylon-6,6. Thermoplastics can show elastic deformation by the distortion of the covalent bonds within the chains after applying some stress. This will cause that the polymers elongate elastically. After removing the applied stress, the material will instantaneously try to recover from this distortion. [20]

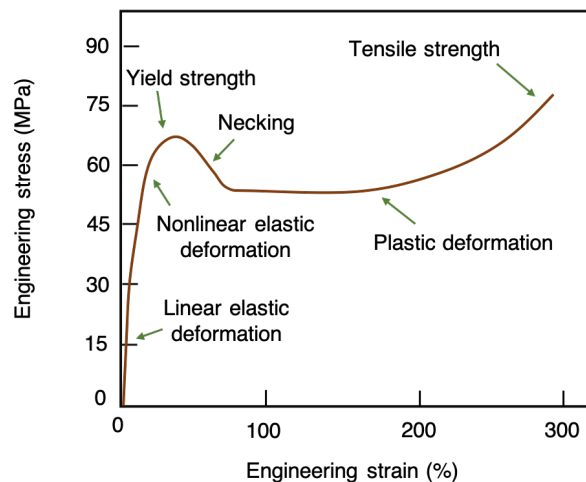


Figure 2. 4. General mechanical behavior of thermoplastics.

Under an applied force, amorphous thermoplastics show a plastic deformation above the yield strength. When this is happening, the polymer chains stretch, rotate, slide, and untangle under the applied force until a permanent deformation occurs. The drop in the stress beyond the yield point can be explained by this phenomenon. When the chains pass from being extremely tangled to being untangled and straighten when the stress is sufficiently high. To allow the slipping of the polymer chains at a lesser stress, necking will occur. Crystallization also occurs at this point. The chains will get closer together and almost parallel. A higher stress will be required to overcome the van der Waals forces that keep the chains together. Once the van der Waals are overcome,

the deformation process will be completed, and fracture will occur. This type of crystallization due to orientation played an important role in the discovery of nylon as a material to make strong fibers. [20]

Because thermoplastic polymers present a viscoelastic behavior, they can exhibit creep (or reptation). This is a time-dependent permanent deformation with constant stress or load. In these types of polymers, stress will decrease under a constant strain, what is called a stress relaxation. Nylon strings in tennis rackets are pulled at a higher tension initially since this tension (i.e., stress) decreases with time. The stress relaxation occurs at a rate which is related to the relaxation time λ . The stress after time t is given by:

$$\sigma = \sigma_0 e^{\left(-\frac{t}{\lambda}\right)} \quad (2.1)$$

where σ_0 , is the original stress. The relaxation time, in turn, depends on the viscosity and, thus, the temperature:

$$\lambda = \lambda_0 e^{\left(\frac{Q}{RT}\right)} \quad (2.2)$$

where λ_0 , is a constant and Q is the activation energy related to the ease with polymer chains slide past each other. Relaxation of the stress occurs more rapidly at higher temperatures and for polymers with a low viscosity. [20]

2.1.3 Deformation of Polyamides

Polyamides can be considered as a crystalline polymer. In this case, there can exist two types of crystalline structures lamellae and spherulites. The crystalline regions of the polymer extend into the amorphous regions as linked chains. After applying a tensile load to the polymer, the crystalline lamellae within the spherulites slide past one another and begin to separate as the linked chains are stretched. The folds in the lamellae tilt until reach the alignment with the tensile load direction. The crystalline lamellae break into tiny units which will slide past one another.

Eventually the polymer will be composed of small aligned crystals united by linked chains and oriented in a parallel direction to the tensile load. The spherulites can also change their shape and elongate in the direction of the applied tensile load. After applying a continuous stress, the linked chains will detangle or break. [20]

2.2. CARBON NANOTUBES

Carbon nanotubes are made of rolled graphene sheets; the latter is a two-dimensional honeycomb structure made of a hexagonal arrangement of carbon atoms. Each single-walled carbon nanotube is formed by only one rolled graphene layer, while in multi-walled carbon nanotubes more than one rolled graphene layers can be found, one around another (see Figure 2. 5). [23] Carbon nanotubes are considered for having extremely high stiffness and unique mechanical properties due to their C-C double bonds. This type of bond is one of the strongest interactions that can be found in nature. This type of bond is classified by its sp^2 hybridization, where three of the valence shell electrons are involved in a C-C double bond. The remaining electron, which is called the π -electron, is freely moving around. Because in CNTs are generally found C-C covalent bonds, they are characterized for having extended π -electron clouds. For this reason, they can show remarkable thermal and electrical properties. [24] In this section we will talk about the atomic structure, the methods that currently exist to synthesize CNTs, and how these two attributes affect their mechanical properties.

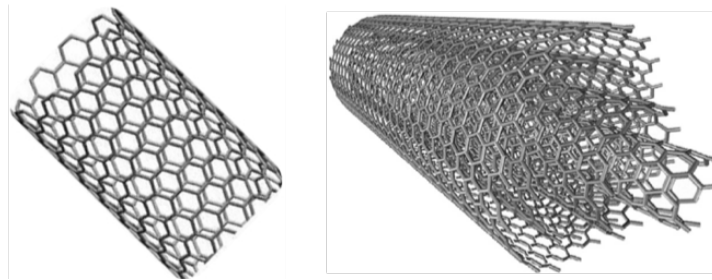


Figure 2. 5. Structure of (a) SWCNTs and (b) MWCNTs.

2.2.1 Atomic Structure of Carbon Nanotubes

The way which the graphene sheet is rolled in order to produce the CNTs can be described in terms of chirality and helicity, using a chiral vector \vec{C}_h or angle θ . [24]

The following equation defines \vec{C}_h :

$$\vec{C}_h = na_1 + ma_2 \quad (2.3)$$

In equation (2.3), n and m are integers that describe the unit vectors a_1 and a_2 (see Figure 2.6). The chiral angle θ determines the amount of twist of the carbon nanotubes. [24] According to \vec{C}_h and θ , a CNT can be classified as a zigzag, an armchair or a chiral nanotube. When $m \neq n \neq 0$, and $0 < \theta < 30^\circ$ could be said that the CNT is chiral. However, if we have that $m \neq n = 0$ ($\theta = 0^\circ$) or $m = n = 0$ ($\theta = 30^\circ$), the CNT could be zigzag or armchair, respectively. Chiral and zigzag CNTs are categorized as semiconductors, while armchair CNTs act as conductive materials showing metallic behaviors. Another parameter that can affect the CNT properties is the amount of the rolled graphene layers. [24]

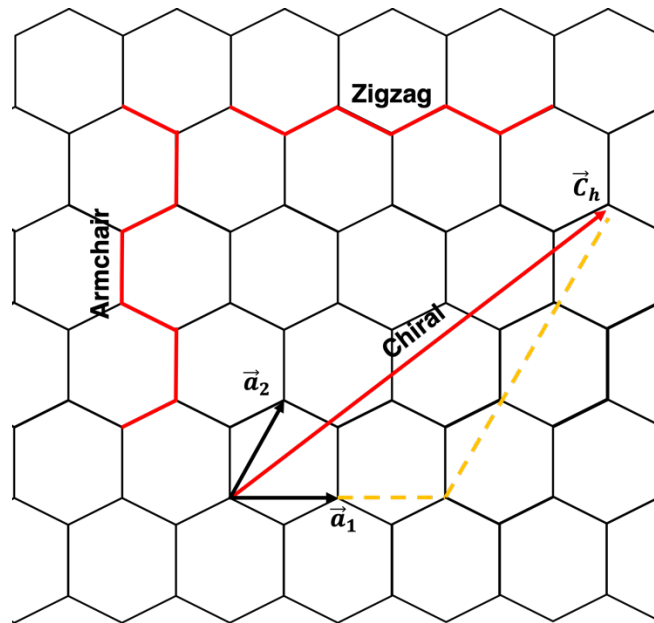


Figure 2.6. Chirality of CNTs.

a. Single-walled carbon nanotubes

Diameters of single-walled carbon nanotubes (SWCNTs) can be found between 0.4-3 nm. Normally, the thickness of the graphene layer is approximately 0.34 nm. [25]–[27] For a given

(m, n) carbon nanotube, the radius of the tube can be calculated using chiral vector integers, m and n , as follows:

$$R_{CNT} = \text{Length of } \frac{\vec{C}_h}{2\pi} = \frac{a_0 \sqrt{m^2 + mn + n^2}}{2\pi}, \quad (2.4)$$

where a_0 is the length of each unit vector. [24] The sp^2 C-C bond length is approximately $b = 0.142$ nm, and therefore $a_0 = \sqrt{3}b$. [24], [28], [29] This type of CNT is widely used for electronic applications because of their semi-conductive and/or conductive properties. [23]

b. Multi-walled carbon nanotubes

Multi-walled carbon nanotubes (MWCNTs) were discovered in 1991 by Iijima et al. two years before the discovery of the SWCNTs. [30] MWCNTs diameters ranged between 3-30 nm. [28] Since MWCNTs consist of a compilation of concentric SWCNTs with different diameters, there are other interactions than the sp^2 C-C covalent bonds. [23] Between each of the CNT cylinders there are secondary (non-covalent) interactions, more specifically, van der Waals forces. Van der Waal forces can be explained using the Lennard-Jones potential, which is described by:

$$V_{LJ} = 4\varepsilon \left[\left(\frac{\sigma}{r} \right)^{12} - \left(\frac{\sigma}{r} \right)^6 \right] \quad (2.5)$$

In equation (2.5), σ [nm] is the distance at which the potential between two interacting particles is equal to zero, and ε [kJ/mol] is the minimum potential acting on the two same particles. Both parameters are exclusive for each material and determine the nature and strength of the bond. [24], [31] In the case of carbon nanotubes, values of $\sigma = 0.3851$ nm and $\varepsilon = 0.4396$ kJ/mol, have been determined for their non-covalent interactions. [24] Figure 2.7 shows the Lennard-Jones potential diagram for two interacting carbon atoms.

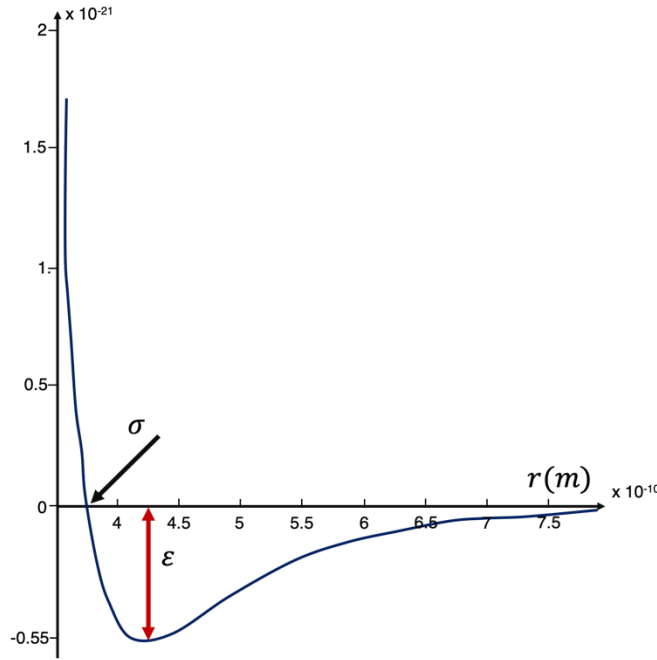


Figure 2. 7. Lennard- Jones potential diagram for two interacting carbon atoms.

The Lennard-Jones force is a weak bonding that results from the Lennard-Jones potential. This force become strongly repulsive when two particles are very close; however, when these two particles are far way, it becomes slightly attractive. The critical distance (r_0), which is the distance when the force is equal to zero, can be obtained from:

$$F_{LJ} = \frac{dV_{LJ}}{dr} = \frac{4\epsilon}{r} \left[-12 \left(\frac{\sigma}{r} \right)^{12} + 6 \left(\frac{\sigma}{r} \right)^6 \right] \quad (2. 6)$$

If $F_{LJ} = 0$, r_0 will be given by $\sqrt[6]{2} \cdot \sigma$ (see Figure 2. 8). After analyzing the Lennard-Jones potential in a MWCNTs system, Kalamkarov et al. found that there could be a range of distance from 0.33 to 0.38 nm between each CNT layer. [24], [31] Thus, it should be considered that by applying an external load on the structure, the locations of atoms with respect to each other change and as result, the Lennard-Jones force changes. [24]

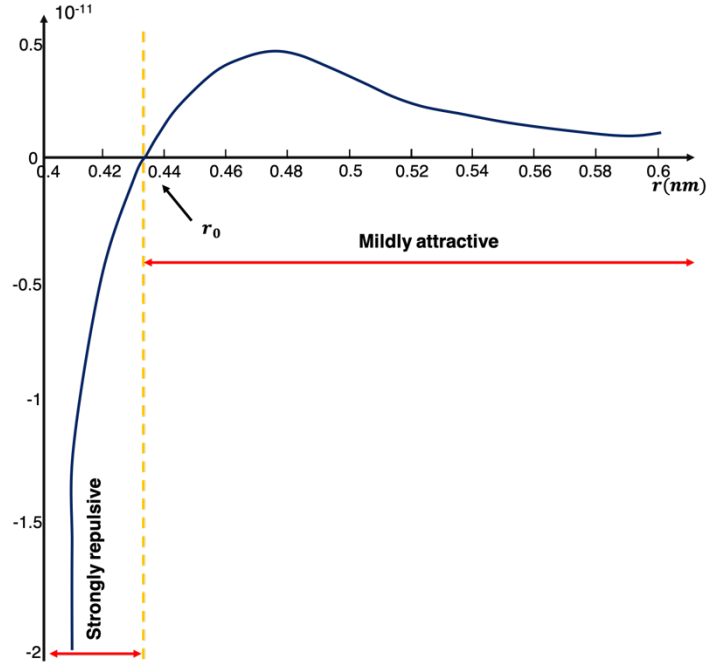


Figure 2. 8. The Lennard-Jones force in carbon nanotubes.

Additionally, interactions between two particles can be described using the Morse potential function:

$$V(r) = \varepsilon [e^{2\beta(\rho-r)} - 2e^{\beta(\rho-r)}] \quad (2. 7)$$

$$F(r) = 2\varepsilon\beta [e^{2\beta(\rho-r)} - 2e^{\beta(\rho-r)}] \quad (2. 8)$$

where β represents an inverse length-scaling factor, and ρ and ε are the equilibrium bond length and displacement energy, respectively. [24] Both Lennard Jones and Morse potentials are used in molecular dynamics simulations and are based on the approximation of two-bodies. [24], [32]

2.2.2 Methods to Synthesize Carbon Nanotubes

Since the first carbon nanotube was synthesized by Iijima et al. in 1991 [30], there have been studies to enhance the CNT production. In this section, some of the most used techniques to synthesize CNTs will be presented.

a. Arc-discharge

Arc-discharge perhaps is the simplest method to synthesize carbon nanotubes at a large scale, however the product can show a high content of impurities. This process requires an ignition between two graphite electrodes in a gaseous atmosphere and low pressure. In order to synthesize MWCNTs, carbon atoms from the graphite evaporate due to the arching process, afterwards the materials cool and condense in a filamentous form on top of the cathode. This method might be SWCNTs selective by using a metal in the anode as catalyst (i.e., iron). [23] Through this method CNT with a length of approximately 1 mm long and diameters between 4 to 30 nm can be obtained. [24]

b. Laser ablation

In order to synthesize CNTs under this method, a pulsed laser vaporizes a graphite target. This process is performed at high temperatures and under an inert gas atmosphere. The formed nanotubes will then be collected in a copper substrate. [24] The final product will be carbon nanotubes that are approximately 100 μm long and have diameters that ranged between 10-20 nm. [24] At end a mixture of both SWCNTs and MWCNTs is produced; moreover, only SWCNTs are obtained if a metal catalyst is used. The average CNT diameters and size distribution will depend on the growth temperature, the catalyst composition and other process parameters. [33]

c. Chemical vapor deposition

This method is characterized for producing industrial amounts of CNTs. [34] This process consists of a hydrocarbon mixture (ethylene, methane or acetylene) or process gases (i.e., ammonia, nitrogen, and hydrogen) reacting over a metallic target, at 700-1000°C, and at atmospheric pressures. [24] CNTs will be formed as result of the decomposition of the hydrocarbon gases. The CNTs diameter will depend on the catalyst particle size. [33] The product is usually collected on a silicon, glass or alumina substrate. [24] There are other methods to synthesize CNTs that could be classified under this category, and they are:

i. Plasma Enhanced Chemical Vapor Deposition (PECVD)

This method allows to obtain vertically aligned tubes for industrial purposes. Here, two parallel electrodes at a high frequency voltage are used to produce a glow discharge to make CNTs grow

on a substrate. [24] Metal catalysts (i.e., iron, nickel, and cobalt) are required in this process, and they will determine the nanotube's diameter, growth rate, wall thickness, morphology, and microstructure. [24], [35] This process will occur under a gaseous atmosphere, that includes but is not limited to C_2H_2 , CH_4 , C_2H_4 , C_2H_6 , CO , are the carbon sources. [24]

ii. Vapor phase growth

In order to obtain CNTs under this method, ferrocene is used as catalyst which will vaporize at low temperatures. Small catalytic particles are formed. The decomposed carbon is absorbed and diffuse into the catalytic metal particles. [24] Generally, SWCNTs obtained by this method have diameters between 2-4 nm, and MWCNTs between 70-100 nm. At the end large amounts of CNTs will be produced. [36], [37]

iii. High Pressure Carbon Monoxide Reaction Method

In this method the metal catalyst, which is usually iron carbonyl in a gaseous state, will be mixed with a flow of CO at high temperature and pressures. This catalyst will decompose and form nanometric metal particles. [24] On the catalyst's surface, carbon molecules react to form CO_2 and carbon atoms, which will then attach and form the carbon nanotubes. [24] This is a selective process and will produce large amounts of SWCNTs with highly variable tube diameters. [24]

2.2.3 Mechanical Properties of Carbon Nanotubes

The remarkable mechanical properties that CNTs can show are strongly related to the type of bonding between the carbon atoms in the graphene layer. The required energy to break only one sp^2 C-C bond in a CNT is approximately 628 kJ/mol. Many investigations have been done, including experimental procedures and simulations, to determine the elastic modulus (also referred to as Young's modulus) for CNTs. It was determined that Young's modulus, for both, SWCNTs and MWCNTs, is between a range of 0.8-1.7 TPa. [24] It was also found that wall thickness, tube diameter and chirality in the CNTs might slightly affect their elasticity modulus. [24] The number of walls in MWCNTs can also affect their dispersion in the matrix and, by consequence, this may create more defect in the samples and decrease the modulus of elasticity.

[18] Another mechanical property of CNTs that scientists have tested is the shear modulus. This property can be evaluated by torsion and/or tensile tests. Similar to the investigations related to the determination of the elasticity modulus, many researchers have studied the shear modulus of CNTs using experimental and simulation procedures. [24] Since CNTs show an isotropic behavior, the values obtained from tensile tests can differ to those obtained from a torsion test. [38] There is a slight difference between the shear modulus of SWCNTs and MWCNTs. For both types of CNTs have been found shear modulus values between 0.1-0.5 TPa. [24] According to Ghavamian et al., the shear modulus decreases with the increasing of the number of walls in MWCNTs. [38]

2.2.4 Non-Covalent Functionalization

Non-covalent functionalization can be reached by polymer wrapping, surfactants or small aromatic molecule adsorption, among other techniques. [23] This process is usually done to improve certain properties of other materials without affecting the carbon nanotube properties. [23] The covalent functionalization of carbon nanotubes requires the rupture of the strong sp^2 bonds between the carbon atoms of their walls, this could affect their mechanical and electrical properties. [23] This type of functionalization primarily involve hydrophobic, van der Waals, and electrostatic forces and requires physical adsorption of suitable molecules onto the sidewall of the CNTs. [23]

2.3. COMPOSITES MATERIALS

Composites are made after merging two or more materials in order to combine their properties. This combination of properties usually cannot be found in the single components. Wood and bones are examples of natural composites. Small or large particles, and/or long or short fibers can be used as reinforcement materials that are characterized for being the structure's load carrier in the composite. In this study we used randomly oriented carbon nanotubes, which can be classified as short fibers (see Figure 2. 9). Since these fibers are short fillers (with a size less than 100 nm), these types of composites are classified as nanocomposites. [24] Composites that use carbon nanotubes as reinforcement are studied to replace alloys in aerospace and automotive applications because of their strength, light weight, coefficient of thermal expansion, resistance

to fatigue, better resistance to corrosion, and their easier fabrication methods. [39] The major constituent in a composite is the matrix and this could be metal, ceramic or polymer materials. The matrix is responsible for binding the CNTs together, transmitting the external applied stress and distributing them to the reinforcement. To accomplish this, the elastic modulus of the reinforcement should be higher than that of the matrix. [24]

2.3.1 Polymer-Matrix Composites

As was mentioned earlier, this work focuses on composites that have polyamide 6 (nylon-6,6) as a matrix. Since usually the matrix has lower melting temperatures, the processing temperature should be determined by them. In general, the polymers with better prospective for aerospace engineering are the thermoplastics with melting temperatures higher than 230°C. [39]

2.3.2 Short-Fiber (Carbon Nanotubes) Reinforcement

Researchers have proven that the elastic modulus of a short-fiber reinforced composite (SFRC) is greatly affected by the volume fraction, aspect ratio and the orientation of the reinforcement. [40] At higher CNT compositions or aspect ratios we can expect higher elastic modulus. Simulations by boundary element method (BEM) have shown that the for a fixed tube orientation, the effective elastic modulus (E_x) increases with the tube's aspect ratio. [41] Even though some applications require aligned fiber composites it is also appropriate to create composites with randomly oriented short fiber reinforcements in case the application is subjected to multidirectional stresses. [39] (See Figure 2. 9). In the case of materials with randomly aligned fibers isotropic behavior could be favored. The elastic modulus of these types of composites, the elastic modulus can be explained by the following equation

$$E_{c-short} = KE_fV_f + E_mV_m \quad (2. 9)$$

In this equation K, the efficiency parameter, depends on the final volume (V_f) and the ration of E_f/E_m . (explain this better) [24] Usually the fibers cannot reinforce a composite from the transversal section, and fracture of the composite at lower tensile stresses tends to occur. The

reinforcement efficiency factor value varies between one for stresses applied parallel to the fibers and zero for transverse loads, in a way that any arrangement of short fiber lays between these two extremes. [24] For instance, reinforcement efficiency for randomly and uniformly distributed fibers within a specific plane and load applies in any direction in the plane is equal to 3/8 and in case of fibers randomly and uniformly distributed within three dimensions in space and stress applies in any direction is 1/5. Industrially, short-fiber reinforced composites are more attractive since the production rates are quicker and they have lower production costs than those of long fiber reinforced composites. [24]

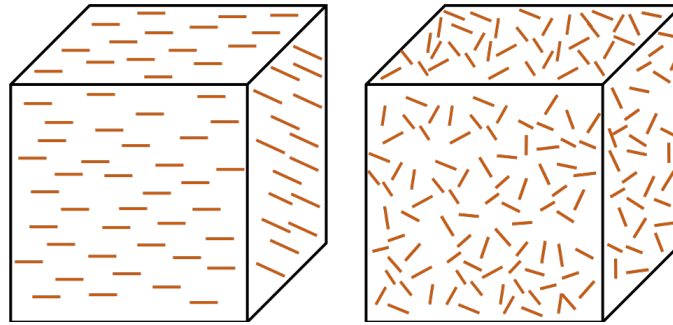


Figure 2. 9. a) Aligned fiber and b) randomly organized fibers in a matrix.

2.3.3 Composite's Behavior at the Interface

Amongst the matrix and the CNTs can be found an interface where there is a discontinuity that is either sharp or gradual. Changes such as the concentration of a component, crystal structure, atomic arrangement, elastic modulus, density, and coefficient of thermal expansion occur at the interface. Some single factors, or a combination of them can affect the behavior of a composite, the factors are the reinforcement component (CNTs), the matrix, and the interface between them. [42] There is a strong correlation between the fiber (nanotube) surface area and the interfacial area, both are practically the same, and the surface-to-volume ratio (S/V) can be defined by:

$$\frac{S}{V} = \frac{2\pi r l}{\pi r^2 l} = \frac{2}{r} \quad (2. 10)$$

where r and l are the fiber (tube) radius and length of the fiber, respectively. It is understood that at smaller r , the fiber's surface area increases. [42] The load transfer will occur at the interface between the tube and the matrix.

An important step in the formation of a composite is the wetting process. Wettability is the capability of a liquid phase to spread on a solid surface. [42] This property can be measured by considering the equilibrium of forces between a drop of liquid and the solid surface it rests on. [42] To lower the system's free energy, the liquid drop will spread and wet the surface. Young's equation explains the forces acting horizontally in the system:

$$\gamma_{SV} = \gamma_{LS} + \gamma_{LV} \cos \theta \quad (2.11)$$

The term γ is the specific surface energy, and the subscripts SV , LS , and LV represent solid/vapor, liquid/solid, liquid/vapor interfaces, respectively. [42] If the contact angle (θ) of a liquid on the tube's solid surface range between $0^\circ < \theta < 180^\circ$ it could be said that wetting occurred. Usually, smaller θ values mean good wetting; moreover, smaller values of θ do not necessarily mean that a strong bonding has occurred. [42]

It is fundamental to understand that wettability and bonding are not the same. While wettability describes the ability of a liquid to spread, it does not mean that there a strong bond between two materials at the interface. Young's equation can be used to analyze how a drop spread on a surface, but it only considers the surface tension in the horizontal direction. However, there is a vertical force, $\gamma_{LV} \sin \theta$, which is normally neglected, and must be balanced by a stress in the solid acting perpendicular to the interface. Young's equation takes in consideration the voids in the solid, but no the precise state of internal stress. The wetting process is fundamental in the polymer-matrix composite fabrication, since the polymer must penetrate and wet, in its liquid state, the reinforcement (i.e., the carbon nanotubes). Usually, thermoplastic polymers have higher viscosity values making wetting processes more complicated. The contact angle (θ), which is a measurement of wetting, depends on factors such as time and temperature of contact, interfacial reactions, stoichiometry, surface roughness and geometry, heat of formation, and electronic configuration. [42]

2.3.4 *Interactions at the Composite's Interface: Mechanical and Physical Bonding*

The components in a composite material are usually chosen because of their individual mechanical and physical properties. Nevertheless, it is important to keep in mind that when two materials are combined, the system will rarely be in a thermodynamic equilibrium. In the system's stabilization process typically will exist a driving force due to the interactions between both components. In the absence of thermodynamic and kinetic information, it is essential to perform experimental studies to understand the behavior of the two components in the system. The manufacturing process can normally implicate interfacial interactions which can change the properties of the components and/or the interface structure. For example, if the fabrication process involves great temperature changes, the difference between the coefficient of thermal expansion of both components might lead to thermal stress of great magnitude. Metal matrices usually deform plastically under great thermal stresses; in contrast polymeric matrices relieve stress by producing microcracking, instead of plastically deforming. There are different types of bonding between the carbon nanotube and the polymer at the interface. Here, we will be only discussed the mechanical and physical bonding types. [42]

In a carbon nanotube reinforced composite, any contraction of the matrix onto a central nanotube would result in gripping of the tube by the matrix. The polymeric matrices usually contract in a radial form at high temperatures. For this reason, gripping of the tube by the polymer occur without the need of forming chemical bonds. The matrix normally penetrates the crevices on the nanotube's surface by liquid or viscous flow or high-temperature diffusion, leading to some mechanical bonding. [42] In Figure 2. 10., we show a radial gripping stress, σ_r . This is related to the interfacial shear stress, τ_i , as

$$\tau_i = \mu \sigma_r \quad (2. 12)$$

where μ is the coefficient of friction, and generally lies between 0.1 and 0.6.

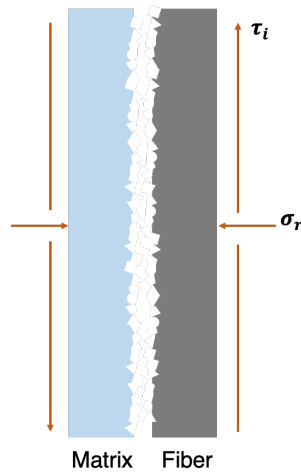


Figure 2. 10. Relation between the gripping stress (σ_r) and the interfacial shear stress (τ_i).

The bond energy is lower in mechanical bonding than in chemical bonding. However, studies have shown that the mechanical gripping of the fibers by the matrix is sufficient to cause an effective reinforcement. [43], [44] Mechanical bonding leads to good load transfer if the force is applied in the parallel direction to the interface. In order to achieve this, complete wetting of the nanotube by the matrix at the interface should occur. Surface roughness can also contribute to the bond strength if the liquid matrix can properly wet the nanotube's surface. Voids are normally formed, because polymer matrices are unable to completely penetrate the asperities on the nanotube's surface (see Figure 2. 11). At the interface of the CNTs/polymer composite system physical bonding such as van der Waals, and hydrogen bonding can also be found. This type of bonding usually has a low bond energy (strength) ranging between 8-16 kJ/mol. [42]

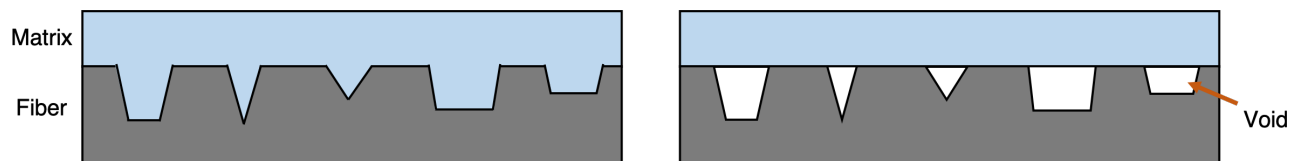


Figure 2. 11. (A) Good mechanical bond (B) poor wetting between the matrix in the liquid state and the filler surface.

2.3.5 Mechanical Properties

Composites are generally fabricated to improve the properties, such as mechanical properties, of the component with major concentration, which is supposed to be the matrix. It is important to

understand that the mechanical properties of a composite materials depend on several features. [24] Some examples are the geometry and the properties of the reinforcement material, the concentration and volume fraction of the reinforcing material with respect to the matrix, the matrix's properties, the homogeneous dispersion of the reinforcing material in the matrix, and the interfacial strength between the reinforcement and the polymeric matrix. As was discussed earlier, CNTs' elastic modulus ranges from 0.3 to 1 TPa and their strength between 10-500 GPa. For this reason, and because they are low aspect ratio and light weight they have become promising materials to be used as reinforcing material in nanocomposites. [45]–[48] Moreover, the composite's mechanical properties depend on some factors such as CNT type, growth method of the CNTs and CNT chemical pretreatment, and composite's processing. In order to obtain favorable mechanical properties in CNT-based nanocomposites materials, the dispersion of the CNTs should be majorly homogeneous.

2.3.6 Melt Pressing Method

In melt processing, carbon nanotubes are mechanically dispersed into a polymer melt (prepared by heating) using a mixer or a compounder [18]. The central idea is to use fluid shear forces to break nanotube aggregates or prevent their formation. This approach is simple and compatible with existing polymer processing techniques such as extrusion, injection molding and compression molding. Therefore, it holds promise for use in large-scale industrial applications.

There have been a few recent studies conducted into the fabrication of CNT/polymer composites using the melt processing method. Jin et al. [19] mixed carbon nanotubes into a polymethylmethacrylate (PMMA) melt in a Laboratory Mixing Molder at 200°C. They then used a hydraulic press to compress the mixture into films.

CHAPTER 3. METHODOLOGY

Fabrication of highly loaded CNTs/PA6 composites with a homogeneous distribution is the objective of this study. In this chapter, materials and methods used to manufacture these composites will be presented. In addition, the importance of parameters such as CNT composition, maximum temperature and applied pressure during the process will be also discussed. Samples were assembled, thermally treated, characterized and tested to determine the elastic modulus and hardness. Moreover, an additional analysis was conducted to determine whether or not polymer degradation was occurring.

3.1. MATERIALS

Commercially available polyamide 6 (0.06 mm thick) sheets were obtained from Goodfellow USA. Both types of CNTs, single-walled and multi-walled, were provided by Bucky USA (Houston TX, United State). MWCNTs were synthesized by the CVD method with a resulting diameter in the range of 15–20 nm, lengths between 1-10 μm , with about 10 to 20 graphene layers with an internal width from 2 to 5 nm. On the other hand, SWCNTs were synthesized by arc-discharged method with a range of tube diameter and length between 2-10 nm and 10-30 μm , respectively. The company reported a CNT purity of $\sim 70\%$, and they were not post-treated or purified.

3.2. SAMPLE PREPARATION

In a previous study conducted in our laboratory by Margie Guerrero and also directed by Prof. Carlos Marín, [49] carbon nanotubes/poly (ether ether ketone) (CNTs/PEEK) composites were fabricated. As part of the results of this previous investigation, it was found an elastic modulus improvement by approximately 35% and 52% in comparison of neat peek for samples containing a CNT concentration of 40 wt% and 60 wt%, respectively. Samples with even higher CNT load (75 wt%) were tested. However, for these samples, an elastic modulus lower than the one for neat PEEK was found. In the latter samples, it was determined that there was not enough polymer to coat all the CNTs. Based on the successful results obtained with PEEK, it was decided to explore fabrication of CNT/PA6 composites with similar CNTs concentrations.

The same approach that was used to prepare PEEK/CNTs samples was used to prepare PA6/CNTs composites. Figure 3. 1 a and b show the CNT/polymer assemblage that was used to fabricate the CNTs/PA6 composites. A sandwich type structure was prepared consisting on fifteen alternating layers, eight layers of PA6 (gray films in Figure 3. 1 a, b and c) and seven layers composed of randomly dispersed CNTs (black particles in Figure 3. 1 a, b and c). It is important to mention that the prepared samples had a sandwich type appearance; however, after the thermal treatment, they ended as homogeneous unlayered composites (see Figure 3. 1 d). In order to pour the CNTs between layers of PA6 and to keep them inside, a sort of envelope was developed. Each envelope consisted of two 35 mm x 35 mm x 0.06 mm PA6 layers held together with Kapton (polyimide) adhesive tape, which was selected for its resistance at high temperatures (see Figure 3. 2).

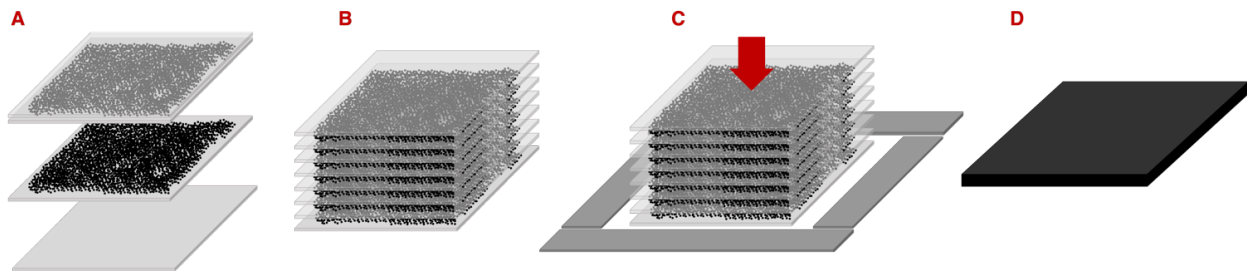


Figure 3. 1. General CNTs/polymer composites fabrication method.

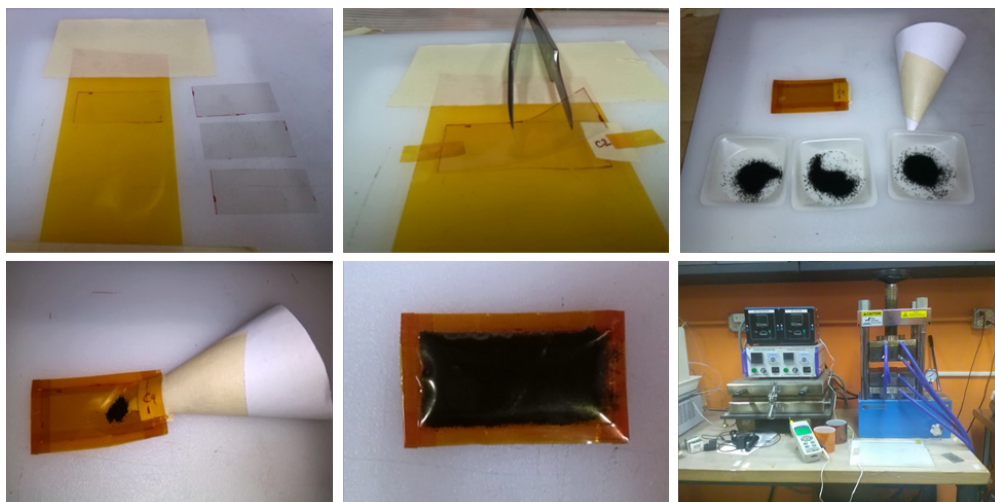


Figure 3. 2. Real representation of the CNTs/polymer composites' fabrication. [49]

A preliminary series of tests were conducted using the following CNT compositions: 40, 45, 50, 55, 60, and 65 wt%. An estimation of the elastic modulus of the samples was obtained by measuring the deflection of approximately 20 mm long samples (L) with the end fixed and force (F) applied to the other end (see equation (3. 1)). In the equation showed below, F (N) is the applied force, L (m) is the length of the beam, E (Pa) is the elastic modulus, I (Kg·m²) refers to the moment of inertia and δ (m) is the beam deflection after applying a force. This was not an accurate method to measure an exact elastic modulus; however, it was valid to determine the structural homogeneity. A tendency of proportional increasing of the sample's elastic modulus with its CNT content was observed. The estimated elastic modulus for the samples containing 40 wt% resulted very low. Nevertheless, the elastic modulus estimation for the samples containing 45 wt% resulted higher than the estimation for the composites containing 40 wt% of CNTs. After this preliminary analysis, CNTs/PA6 composites containing CNTs concentrations between 45-65 wt% were prepared and tested thoroughly using a Dynamic Mechanical Analyzer (DMA) and Vickers Hardness (HV) for more accurate measurements (see Section 3.4).

$$\delta = \frac{FL^3}{3EI} \quad (3. 1)$$

3.3. SAMPLE PROCESSING

There are two important transitions occurring in the polymer when the composite is thermally treated, the glass transition temperature (T_g) and the melting temperature (T_M). Changes from glassy state to a viscous state occurs in the polymer at T_g . If the temperature is increased until the polymer's T_M , the polymer chains will be able to thermally move and rearrange. In this case, crystallization can occur if there is a slow cooling rate after the composite have reached the polymer's T_M . In previous experiment performed with PEEK [49], three different heat treatments for the CNTs/PEEK composites were considered. The first treatment consisted on increasing the temperature at a rate of 4.5 °C/h until reach PEEK's T_g (160 °C) and maintain this temperature for four hours, and subsequently decrease the temperature at a rate of approximately 60 °C/h room temperature. The samples resulted from this thermal treatment were not satisfactory because the polymer did not wet the CNTs. The second treatment consisted on increasing the temperature at

a rate of 4.5 °C/h until PEEK's T_g , this temperature was held for four hours to ensure homogeneity in the heating process, then the temperature was increased at the same rate until 240 °C and the temperature were kept constant for four hours. Then the sample was cooled down at the same rate of the previous thermal treatment (60 °C/h). In this second treatment, better looking samples were obtained; however, delamination, poor incorporation of CNT in the polymer matrix and fragility was observed. The third treatment explored was similar to the previous one, but this time the temperature was increased up to 380 °C, which is higher than the PEEK's T_M ($T_M \approx 340$ °C), instead of 240 °C. After that, the system was also cooled at a rate of 60 °C/h until room temperature. Similar to Tishkova et al., the final composite treated under this condition resulted with a homogenous aspect, the polymer was found to be interacting with the CNTs and the samples were sufficiently strong to stand DMA mechanical characterization. Samples resulted with an elastic modulus of 279 MPa. Even though the samples were more compacted and there was found almost no delamination using this last treatment, the CNTs and the PEEK were not completely combined. Reaching the conclusion that the applied pressure during the heat treatment should be incremented.

The samples treated in the previous study were initially processed applying low pressure provided by four clamps. However, determining an accurate pressure level was difficult (see Figure 3. 3). Composites showed a low elastic modulus (279 MPa), in comparison with the neat PEEK, due to high porosity. After a deep analysis, it was found that a pressure increment during the thermal cycle might decrease the porosity in the final sample for better mechanical response.



Figure 3. 3. First hot press used to fabricate CNTs/PEEK composites. [49]

Afterwards, the samples were processed in a hydraulic hot press machine, with a specific and accurate amount of pressure (see Figure 3. 4). After applying a pressure of 5 MPa during the thermal treatment, reaching a temperature above the polymer's T_M , it was found a reduction of the sample's thickness, better distribution of CNTs in the polymer, and an elastic modulus of about 3.07 GPa. Finally, the CNTs/PEEK samples in the previous research were processed above the polymer's T_m and with an applied pressure maximum of 15 MPa. Samples showed even better homogenization and an elastic modulus improvement by 115% in comparison with the neat PEEK.

The analysis from the previous study was taken in consideration to fabricate the CNT/PA6 composites of this investigation. In the present study, CNT/PA6 composites were processed with a similar thermal treatment as the one that was used to fabricate PEEK/CNTs composites but adapted to PA6 melting point.

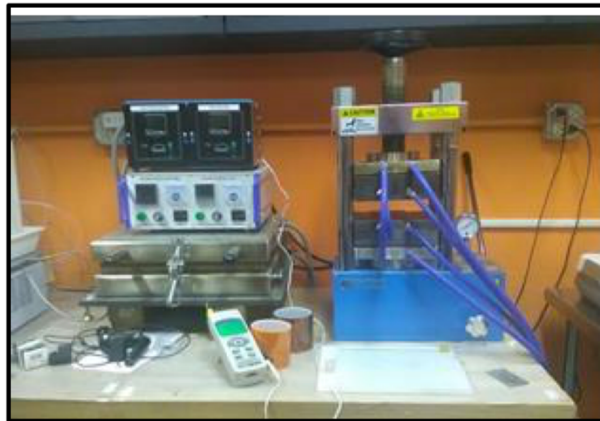


Figure 3. 4. First and second hot press machine used for the composites' manufacturing. [49]

All the manufactured samples on this study were thermally treated in the hydraulic hot press machine, Col-Int Tech (CIT-LPM-H40T2), at two different maximum temperatures, at 280 and 300 °C. Both temperatures are above of PA6's T_M ($T_M \approx 220$ °C), and the reason to use these temperatures was to get similar results that were obtained for PEEK/CNTs composites but at the same time, it was of interest to find the maximum temperature where the composites can be processed without degradation of the polymeric matrix. These temperatures were also chosen because they are in the temperature range typically used to process nylons (260-327 °C). Additionally, two different pressures were applied during the heating process, 5 and 10 MPa. The

purpose of applying pressure to the sample during the heating processing is to achieve a homogeneous dispersion of the CNTs into the matrix. The following heating process was used for the fabrication of CNT/PA6 composites. First, the temperature was raised at a rate of 5 °C/h until the PA6's T_g , 147°C, was reached. Once the system reached T_g , the temperature was kept constant for two hours. After that, temperature was increased at 5 °C/h up to 280 °C. The system was programmed to maintain that temperature, 280 °C, for four hours. The purpose of keeping the system at 280 °C for four hours is to ensure the entire wetting of the CNT surface with the polymer and the redistribution. Lastly, the system temperature was decreased until 30 °C at a rate of 5 °C/h (see Figure 3. 5). To warrant that melt polymer does not spread off, samples were processed limited by a 0.30-0.39 mm thick stainless-steel spacer (see Figure 3. 1 c).

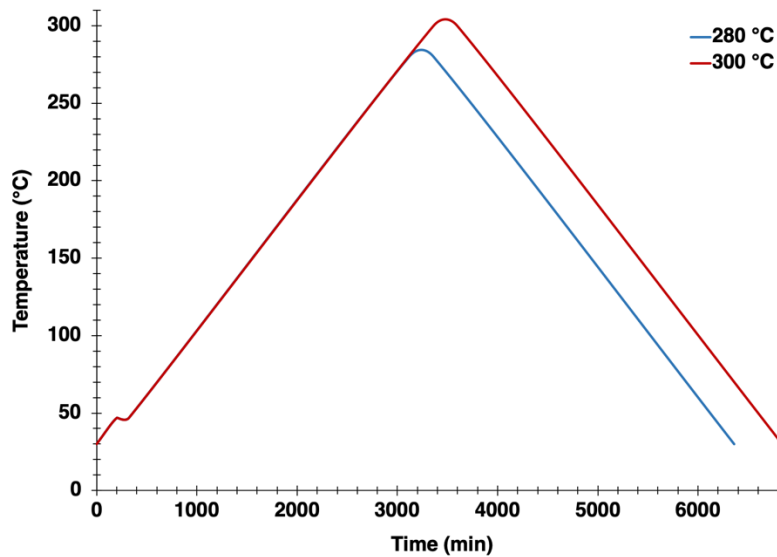


Figure 3. 5. The two heat treatments used to fabricate CNT/PA6 composites, at 280 °C and at 300 °C.

3.4. COMPOSITE ANALYSIS

A scanning electron microscope (SEM Zeiss/LEO 1530) was used to obtain micrographs of all composites. ZEISS software was used for image processing. Each image was obtained with 3 kV and a working distance between 3-4 mm. To determine the Vickers Hardness of each composite a Tukon 1102, from Wilson company, was used. The load applied during this test was 25 grams force (gf) and the time of indentation were 10 seconds.

To determine the HV value the following equation was used:

$$HV = \frac{2 \cdot \sin\left(\frac{\theta}{2}\right) \cdot F}{d^2} \quad (3.2)$$

where F (kgf) is the applied force, $\theta(^{\circ})$ is the angle in the diamond tip (136°), and d (mm) is the average distance between the two diagonals in the indentation (see Figure 3. 6) The units resulting from this equation are kgf/mm²; however, all the HV values were converted to MPa multiplying by the gravitational acceleration force (9.80 m/s²). Samples of approximately 15 mm x 10 mm were mounted in epoxy resin (leaving the cross-sectional area on the top part) and polished before each test. All indentations were made in the cross-sectional part of each composite. To measure the distance of each diagonal, an optical microscope (MTC-01) connected to a camera was used. Each distance was measured using ISC Capture software with a calibrated length scale.

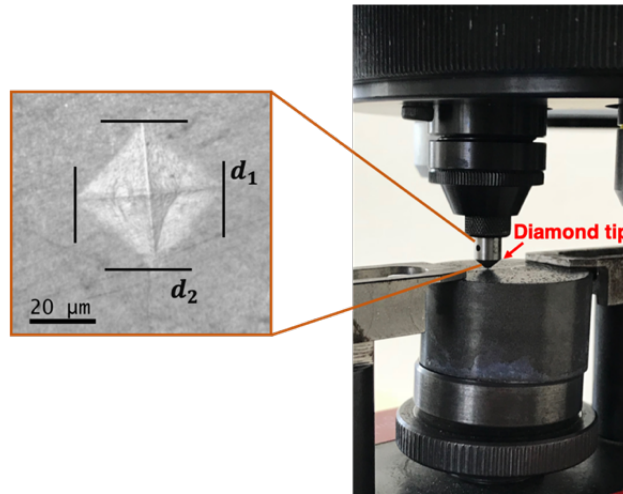


Figure 3. 6. Vickers Hardness test and micro-indentation.

For tensile tests, a TA RSA3 dynamic mechanical analyzer (DMA) was used (see Figure 3. 7). A dynamic strain sweep test was completed for each composite. Tested samples were cut with a length between 20-30 mm and a width of approximately 6 mm. The data was recorded in a strain range between 0.01-0.1 % at room temperature (25°C). For each composite a frequency of 1 Hz was applied, and the force was constantly increased. TA Orchestrator software was used to

record the data. In order to determine if there was or not polymer decomposition, a Thermalgravimetric Analysis (TGA) was performed for both, neat PA6 and for CNTs/PA6 composites. Both temperatures, 280 °C and 300 °C, were tested in this analysis and they were kept constant for only two hours and the temperature was increasing at a rate of 20 °C/min.

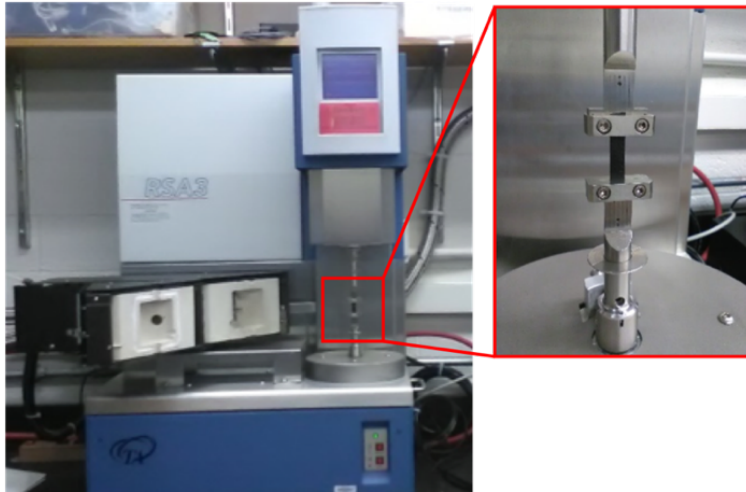


Figure 3. 7. Dynamic Mechanical Analysis.

CHAPTER 4. CARBON NANOTUBE/POLYAMIDE 6 STRUCTURAL CHARACTERIZATION

One of the most important analysis in this study was the characterization of the CNTs/PA6 composites microstructure to determine whether or not the polymer interacted with the CNTs. In order to accomplish this, SEM micrographs were collected and analyzed. In addition to that, since high temperatures were reached during the thermal treatment of the composites, it was important to understand what was happening with the polymeric matrix during the thermal treatment. For this reason, a PA6 decomposition analysis were performed. In this chapter, the composites' microstructure and thermal behavior will be presented.

4.1. MICROSCOPY

Figure 4. 1 shows multi-walled and single-walled carbon nanotubes, respectively at different magnifications. It is hard to observe impurities such as amorphous carbon or metal catalytic traces if any.

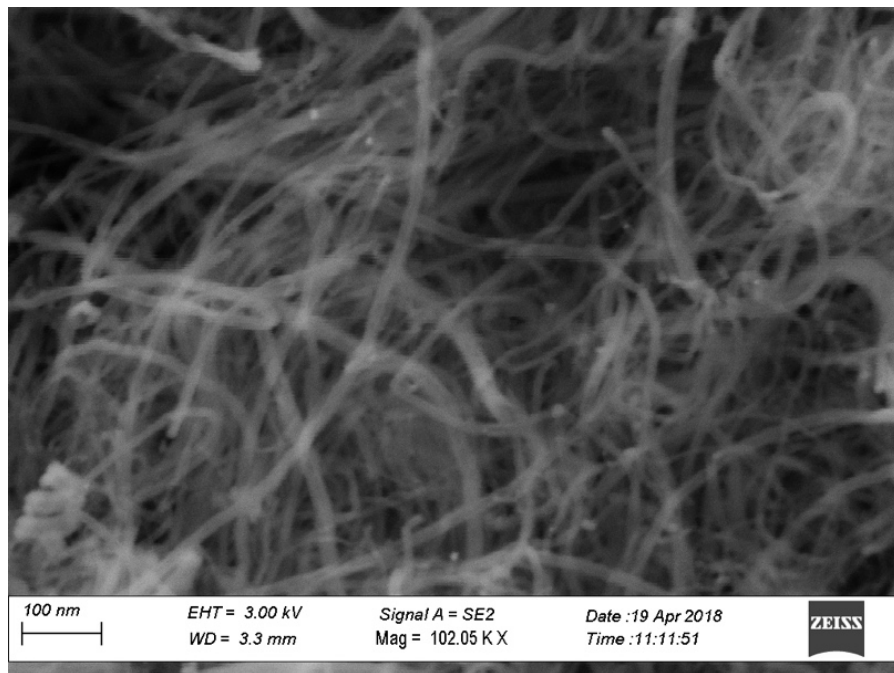


Figure 4. 1. Preprocessed carbon nanotubes.

Figure 4. 2 and Figure 4. 4 show both, MWNT/PA6 and SWNT/PA6 composites, respectively from the sample's cross-sectional area after fracture without polishing. No delamination is showed, which indicates that has occurred integration of the CNTs within the matrix. Similar results were obtained for CNT/PEEK composites in previous studies conducted with PEEK. [49] Figure 4. 3 (a), (b) and Figure 4. 5 show the CNTs/PA6 composites at high magnification, where the reptation of the polymer around the CNTs can be observed. The contrast in the image works as an indicator that there is occurring and interaction between the CNTs and the matrix. The bright sections represent PA6, and the dark ones represent the CNTs. Figure 4. 3 (b) presents accumulation of polymer in some regions (upper right side and middle left side of the image) which indicates that there is no a homogeneous dispersion of the CNTs in this sample. On the other hand, Figure 4. 5 shows a more homogeneous dispersion of the CNTs than the figure previously mentioned. In general, tubes surrounded with bright contrast are showed in both figures which is an indicating that the polymer traveled around the CNTs.

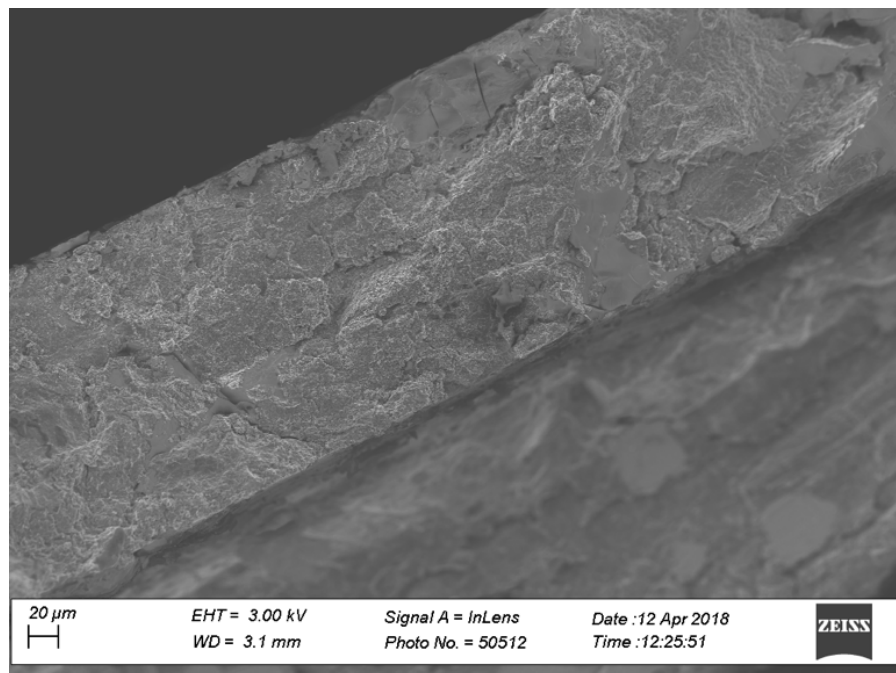


Figure 4. 2. MWCNT/PA6 composites' cross-sectional area after fracture without polishing.

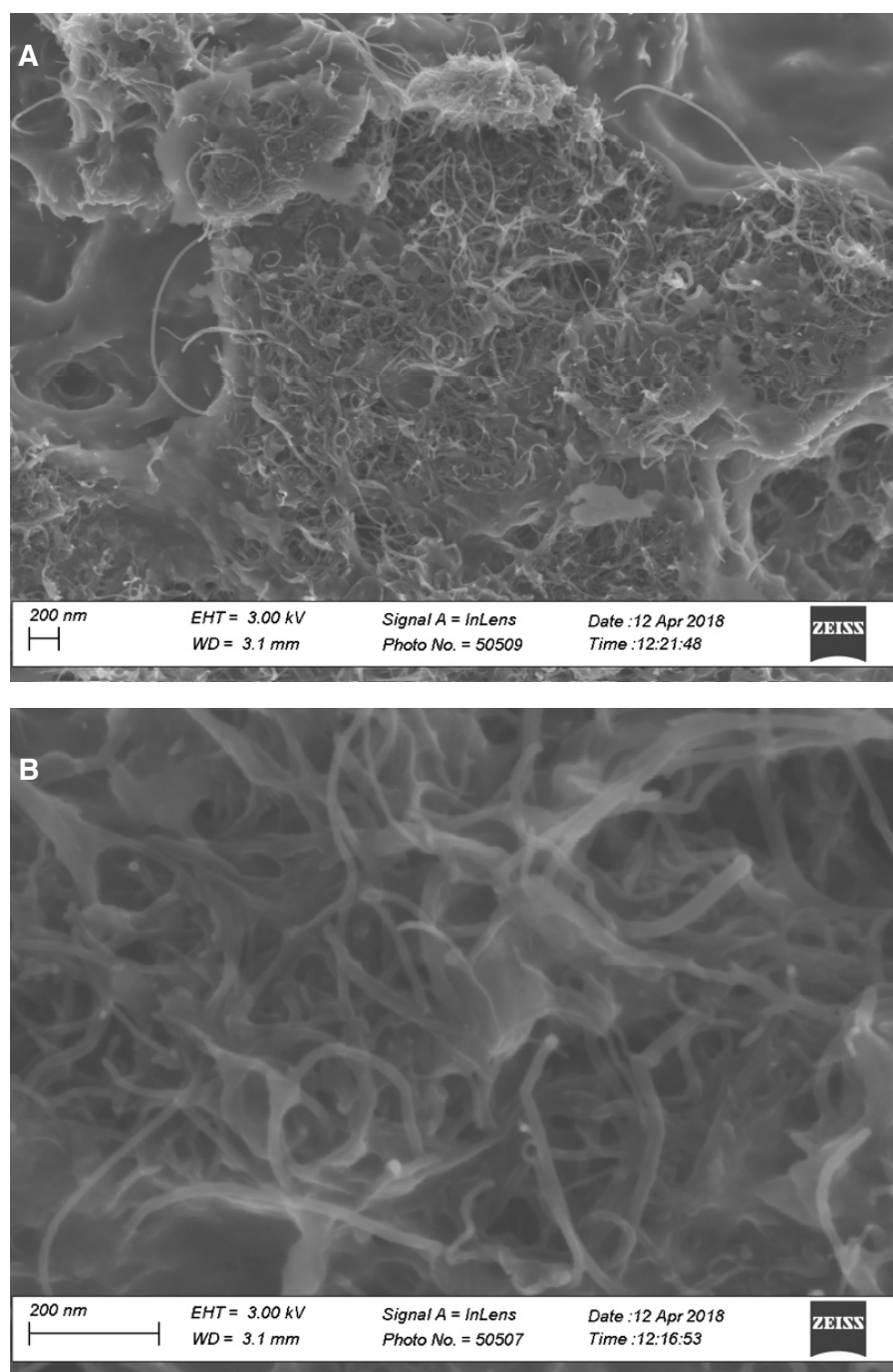


Figure 4. 3. MWCNT/PA6 composites at high magnification.

Different methods to obtain an effective CNT-polymer interaction have been reported. Zhao et al. reported PA6/CNT composites produced by in situ polymerization of PA6. They used both, pure and carboxylates MWCNTs. CNTs were dispersed in a solution containing ϵ -caprolactam and water, then more ϵ -caprolactam was added to the solution to obtain 0.5 wt% MWCNT (or

MWCNTCOOH)/PA6 composites by a typical PA6 hydrolytic polymerization. They chose that CNT concentration (0.5 wt%) because no significant improvements were obtained at higher CNTs loadings by simple melt compounding. These studies confirmed a good dispersion of the CNTs in the matrix by the X-ray scattering (USAXS) data. They reported SEM and TEM images showing good dispersion of CNTs, both MWCNTs and COOH-MWCNTs. [50] In contrast to the study performed by Zhao et al., composites with higher CNT's concentration (45-65 wt%) and showing better interaction within the PA6 and the CNTs were reported in this research. However, in the study performed by Zhao et al., researchers were not able to report composites with CNT's concentration higher than 0.5 wt%, because the PA6 in-situ polymerization process did not allow them to reach higher concentration than that one. In addition, they only reported non-functionalized CNT/PA6 composites with a relatively good dispersion of the filler into the matrix. Additional experiments using CNTs as fillers and the melt compounding method, similar to one presented here, have been done recently. Brosse et al. studied MWCNT/PA6 film composites prepared by melt compounding using a range of concentrations between 0-10 wt%. They reported similar SEM images of non-functionalized MWCNTS well dispersed to the ones reported in this study. [51]

Moreover, Andrews et al. studied the dispersion of multi-walled carbon nanotubes/ polymer films fabricated by high shear mixing using different matrices such as poly(propylene), polystyrene, and HIPS & ABS. The filler content used for the researchers ranged between 0.5 - 5.0 vol% for each matrix. They assigned a value in the range 1 to 10 to evaluate the dispersion of the fibers. The value 1 means poor dispersion and 10 corresponds to the absence of agglomerates and a uniform fiber distribution. The researchers reported good a dispersion of MWNTs under this method; however, in some cases, the action of high shear mixing resulted in their rupture. [52] Further on, Thostenson and Chou studied the CNT dispersion into a polystyrene fabricated by high shear mixing using a micro-scale twin-screw extruder. The studied film composites had a concentration of 5.0 wt% CNTs. The researchers reported well dispersion of carbon nanotubes into the polymer and an efficient wetting process by the matrix. Their TEM micrographs showed cracks interacting with the nanotubes. According to the researchers, the presence of fracture tubes and evidence of the matrix adhered to those fracture nanotubes indicates good wetting of the polymer. [53] It is important to mention that, in this study, lower concentrations of CNTs were not favorable, because this increased the probability of having non-

uniform CNT distribution in some regions of the final processed film. Our method, therefore, works best for highly loaded polymers.

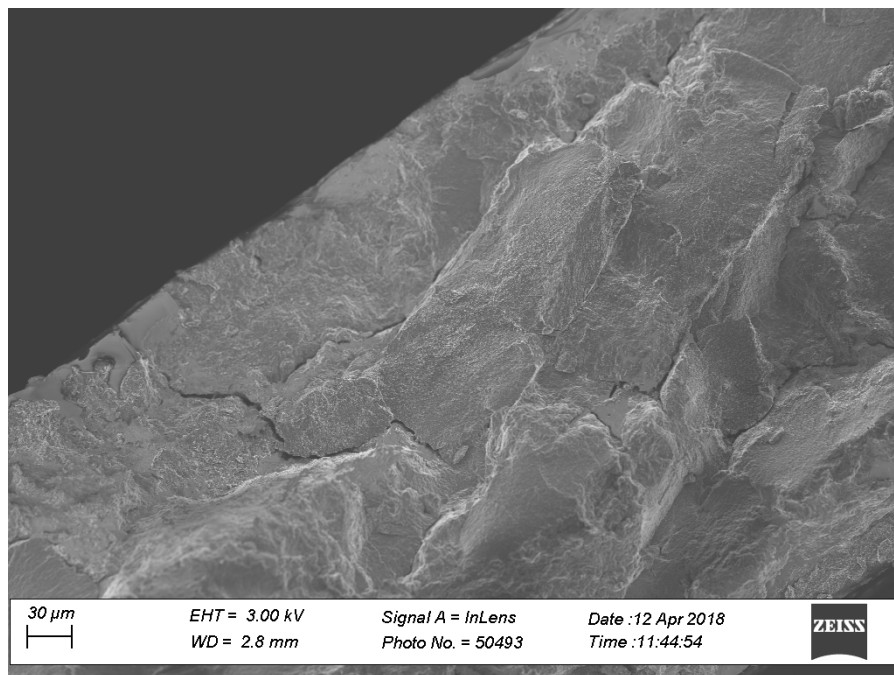


Figure 4. 4. SWCNT/PA6 composites' cross-sectional area after fracture without polishing

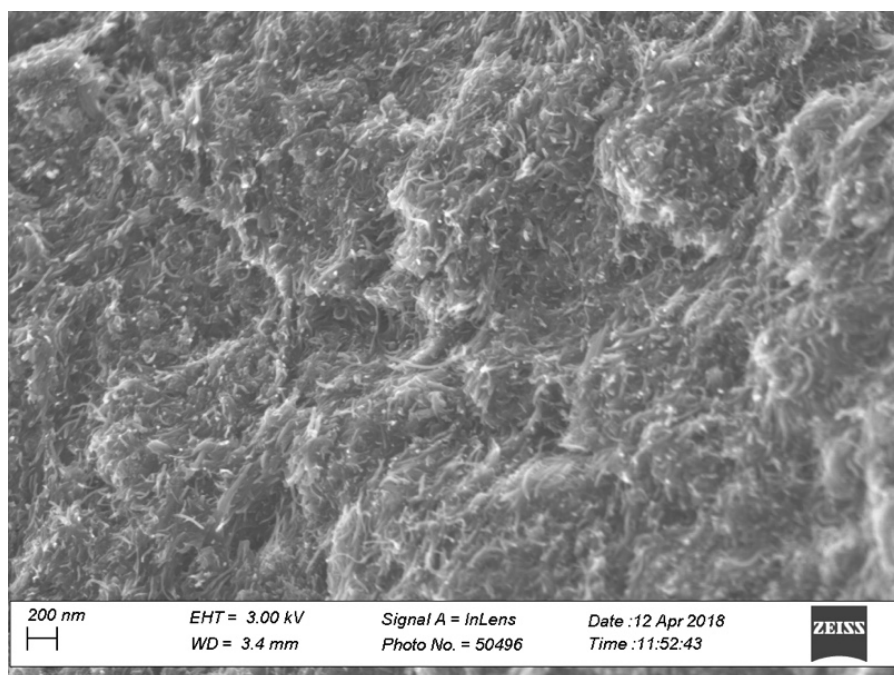


Figure 4. 5. SWCNT/PA6 composites at high magnification.

Figure 4. 6, Figure 4. 7, and Figure 4. 8 show defects in composites containing 55 wt% MWNTs or SWNT and processed at two different pressures, 5 and 10 MPa. These defects are not found with PEEK [49] and could be attributed to possible excess of water in the samples or/and degradation of PA6 due to the explosion of prolonged time at high temperatures. The latter assumption will be in detail explained in section 4.2, page 45. Juan Li et al. conducted a drying process for the CNTs and the PA6 before preparing the composites. [54] This is a process that was not performed before the sample preparation. Having trapped water in the polymer could be a possible explanation of these defects that resulted in all our samples. Less defect content can be observed in those samples processed with an applied pressure of 10 MPa (see Figure 4. 7) compared to those films treated with an applied pressure of 5 MPa (see Figure 4. 6). A similar behavior occurred in the Henriksson and Berglund work who were studying melamine formaldehyde (MF)/micro-fibrillated cellulose film composites. The researchers found smoother surfaces in the composites due to the applied compression pressure during the processing. They argued that the compression step helped the MF to enter and filling some of the porosity in the sample. [55] In addition to obtain a well distribution of filler in the matrix, the application of pressure during the sample processing can help to improve the wetting process of the CNTs with the matrix. [56] It is important to reduce the defects on the composite films, because they mean that there is stress concentration and thus the sample can easily fail.

In contrast to this study, an extremely low amount (almost none) of defects were observed in CNTs/PEEK composites fabricated in our laboratory. However, it is difficult to have a valid comparison since PEEK and PA6 behave completely different. Moreover, comparing the results obtained in this study with the ones reported by Bacsá et al, which are the basis of this study, they showed better CNTs dispersion than here. However, it is important to mention two points, the first one is that in this study the CNTs were not dispersed in acetone before the composites' fabrication. Bacsá et al. mentioned in their article that they previously mixed the CNTs in acetone in order to obtain a better dispersion. [18] As was mentioned before, in this project was desired to keep the manufacturing process as simple as possible without the necessity to use any kind of solvent. The second point is, even though Bacsá and coworkers do not specified the concentration of CNT in their experiment, their images showed a much lower amount of CNTs than the ones used in this study. [18]

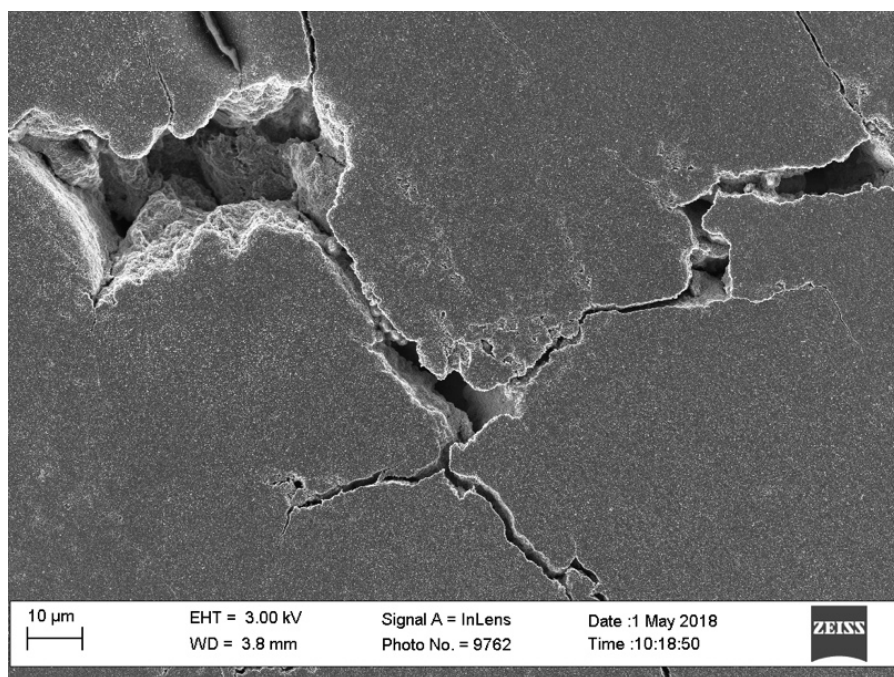


Figure 4. 6. 55 wt% MWCNTs/PA6 composites processed with an applied pressure of 5 MPa.

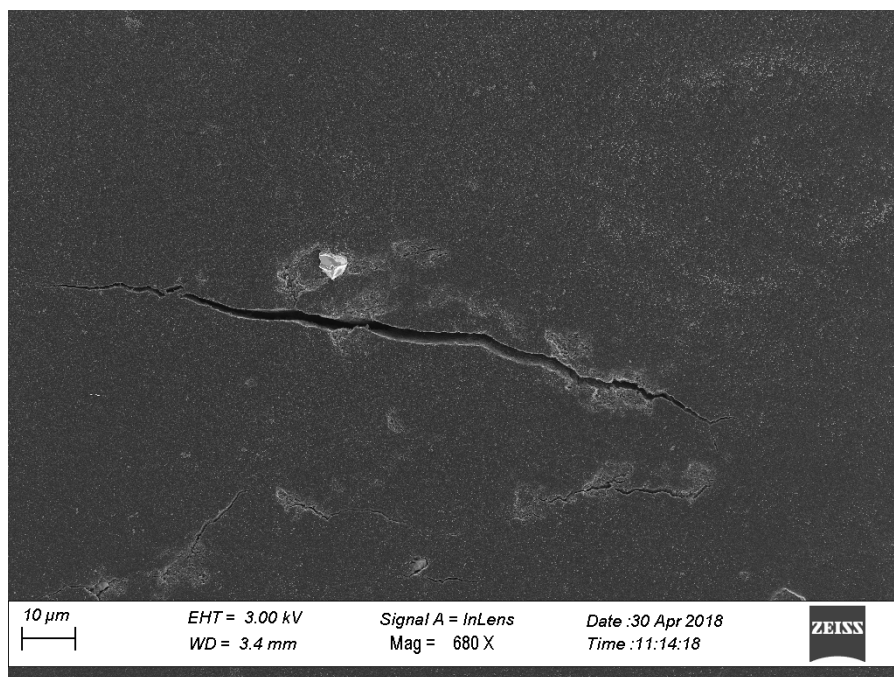


Figure 4. 7. 55 wt% MWCNT/PA6 composites processed with an applied pressure of 10 MPa.

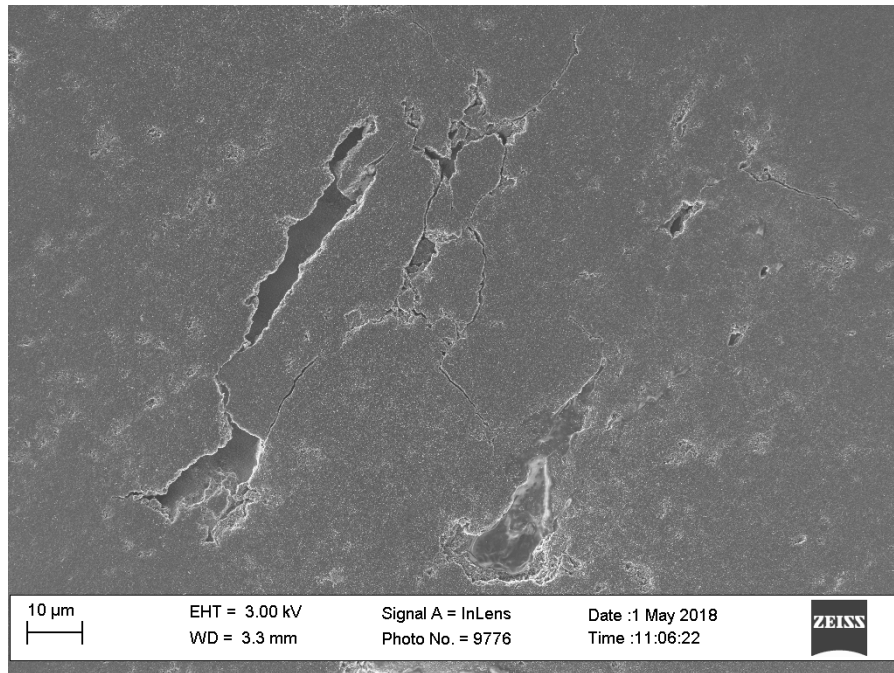


Figure 4. 8. 55 wt% SWCNT/PA6 composites processed with an applied pressure of 5 MPa.

4.2. THERMAL GRAVIMETRICAL ANALYSIS

Figure 4. 9 shows neat-PA6 thermal degradation at (a) 280 °C, and at (b) 300 °C. The continuous red line refers to the degradation that was occurring under nitrogen atmosphere, and the choked green line means that it was occurring under air atmosphere. The continuous blue line indicates the ramp of temperature used during the heating process. At 300 °C the degradation of PA6 is higher than at 280 °C under both atmospheres, air and nitrogen. For both temperatures, PA6 degradation was higher under air atmosphere than under nitrogen, this is due to the oxides that are formed when the polymer is heated in the presence of air. The thermal process at high temperatures under air atmosphere can promote the thermos-oxidation which is an important factor in the decomposition of PA6. [57], [58] Earlier was mentioned that water storage could be a possible explanation for the formation of defects in the samples. This water storage can also explain the abrupt mass decreasing at the beginning of each curve.

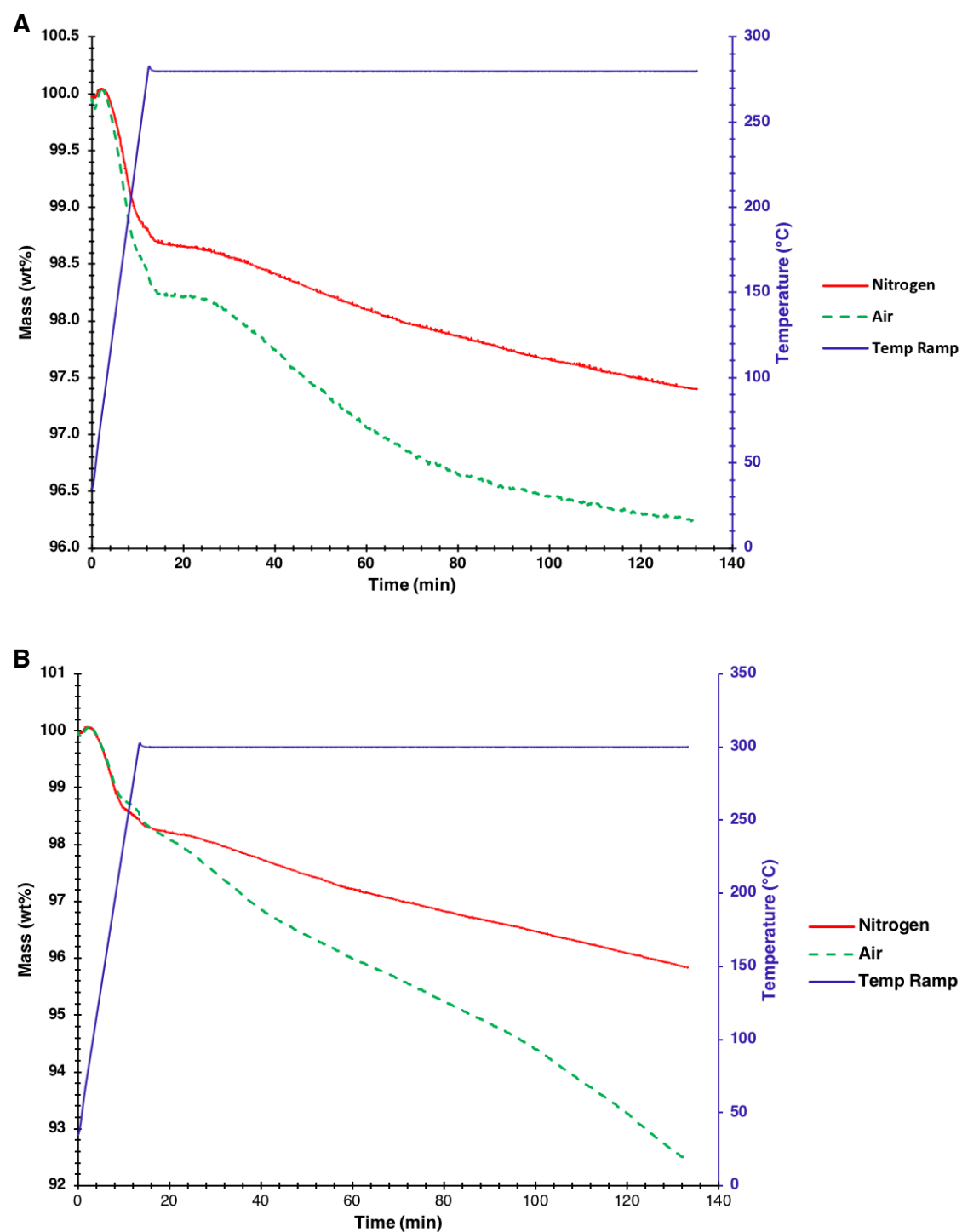


Figure 4. 9. Thermal degradation under nitrogen and air atmosphere of neat polyamide 6 a) at 280 °C and at b) at 300 °C.

Thermal decomposition of polyamides has been extensively studied and there are some proposed mechanisms to explain its behavior under high temperatures. Straus and Wall studied nylon 6 (also known as PA6) degradation under high temperatures and they identified high concentration of products such as CO₂ and H₂O [57], and minor products such as H₂, CH₄, and CO. [57] Different decomposition mechanisms have been proposed. Some researchers have concluded that there are two types of reactions occurring in PA6 thermal degradation under air atmosphere: primary reactions which occur below 300 °C and secondary reactions which occur above 300 °C. As part of the initial step in PA6 decomposition, a homolytic scission of the N-alkylamide bond is suggested. Primary amides, nitriles, isocyanate, nitriles, vinyl groups, and alkyl chain ends are produced from these first reactions (see Figure 4. 10 a). [59] It is also known that this initial step can also compete with other mechanisms depending on the experimental conditions. Hornsby et al assumed that peptide bond hydrolysis is predominant in presence of water. [57], [60] Ref 28 from suggested that cyclic amides can also be produced as primary routes in the thermal decomposition of the generic skeleton of all polyamides. [61]

During secondary reactions, more complex products such as ammonia, cyclic compounds including ϵ -caprolactam (monomer used to synthesize PA6) and others are produced. Zhao et al proposed a pyrolysis mechanism for PA6 decomposition and some possible products from secondary reactions that might be occurring above 300 °C were identified (see Figure 4. 10 b). [62] However, they reported that the main PA6 weight loss comes from sizable quantities of carbon dioxide, carbon monoxide, hydronitrogens, hydrocarbon, and water, at a temperature range of 400-500 °C. Furthermore, mass spectroscopic analysis has showed that, in general, all polyamides decomposed generating water, carbon monoxide, carbon dioxide, and hydrogen cyanide. These same results demonstrated that, in secondary reactions (above 300 °C), hydrocarbons, ammonia, aromatics, alkenes, cycloalkenes, ketones and nitriles can be produced; results which concur with the previously ones reported. [59]

Moreover, Smith et al. suggested a possible re-equilibration of caprolactam, leading the formation of cyclic oligomers, at the beginning of the thermal decomposition of PA6. [63] Results from this study showed that PA6 can undergo to ring-chain equilibrating reactions below the polymer's melting point. Generally, cyclic oligomers have a T_M 20-30 °C higher than PA6, whereas linear oligomers have a T_M 20-30 °C lower than PA6. [64]

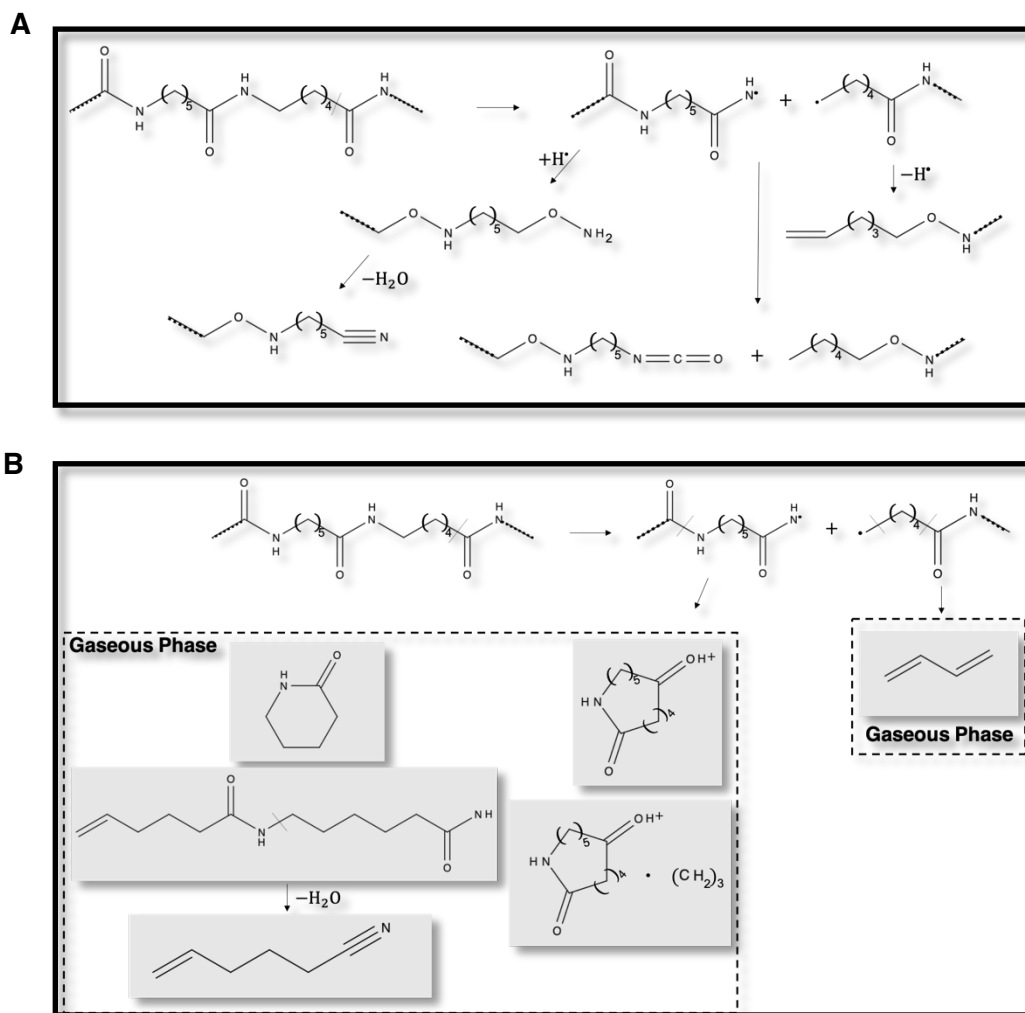


Figure 4. 10. Polyamide 6 proposed decomposition mechanism by a) Levichik et al. and b) by Zhao et al.

Additionally, when PA6 is heated for an extended time at 300 °C, some functional groups such as carbonyl and secondary amines could be branched, which can form crosslinks giving step to a gelling phenomenon. [57], [60] Also, CO₂ can be produced if PA6 is heated for a prolonged time under an oxidative atmosphere. [65] Pagacz et al demonstrated that bio-polyamides can produce small volatile compounds after being heated for approximately 50-60 min. [59] After explaining all these possible reaction mechanisms that occur when PA6 is treated at high temperatures for a long period of time, it can be said that PA6 degradation is the principal reason of getting significant amount of defects in the CNTs/PA6 (presented in the previous section) composites fabricated in this study.

On the other hand, some researchers have reported that, under inert atmosphere, PA6 thermal degradation can occur in three steps [66] and some others have concluded that mass loss can occur in only one step. [59] Pagacz et al studied the thermal degradation of bio-polyamides under inert gas, results showed that, polyamide degradation begins at 360 °C and a wide range of compounds such as large fragments of the PA general skeleton and cyclic amines were identified. Compounds with low molecular weight such as H₂O, CO₂, CO and NH₃, were not found, because there was no oxygen during the treatment. According Levchik et al., most of the products from the PA6 decomposition reactions volatilize at a temperature range of 280-450 °C. [60] For this reason, it can be concluded that the major PA6 decomposition step occurs within this range.

Figure 4. 11 shows the thermal degradation process for SWNT/PA6 composites at (A) 280 °C and at (B) 300 °C. At 280 °C, thermal degradation occurs faster under air than under nitrogen atmosphere. However, at 300 °C the decomposition rate of the samples under both, air and nitrogen, is almost the same. It has been demonstrated that CNTs can delay the degradation of the polymer due to the thermos-oxidation mechanism. However, in the case of functionalized CNTs the degradation temperature of the composites can be lower than the temperature for the composites containing non-functionalized CNTs. [54] Juan Li et al. studied the thermal degradation of pristine-(pure) and functionalized-MWNT/PA6 composites under both, air and nitrogen atmosphere. They prepared composites containing 1.0 wt% of MWNTs by melt blending using the extrusion technique. As part of their research, they tested the thermal properties of both p-MWNTs and f-MWNTs in a temperature range of 50-700 °C. They found only 5% weight loss for p-MWNT at 600°C while for f-MWNTs, they found two-step between 200-500°C, the first step (at 283 °C) is due to the degradation of the functional groups attached on the CNTs surface and the second one (at 440°C) is from the CNT which is at a lower temperature than for p-MWNT due to the bond alteration. [54] For neat PA6, Juan Li et al. found only one-step decomposition under nitrogen atmosphere (between 300-400°C). Meanwhile, under atmosphere, the researchers found that the composites showed two-step decomposition (at 535 °C). For p-MWNT/PA6 composites, the decomposition behavior at air atmosphere is very similar to the one for neat PA6. Moreover, under nitrogen atmosphere, two-step decomposition was found for p-MWNT/PA6 which is different from the behavior of neat PA6 under this same atmosphere. They found that the degradation temperature increased with the increasing of MWNT content. [54]

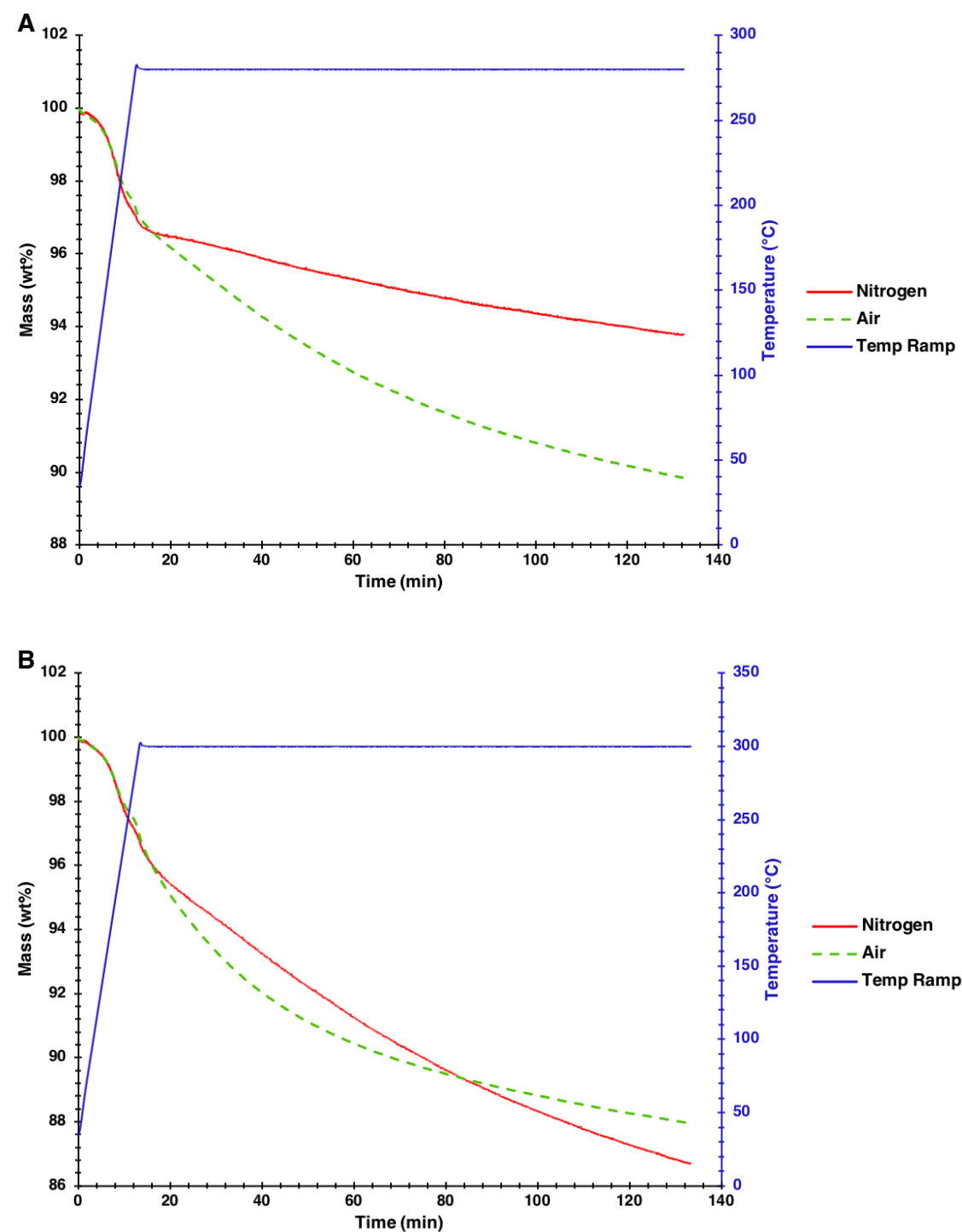


Figure 4. 11. Thermal degradation in nitrogen and air atmosphere of SWNT/PA6 composites a) at 280°C and at b) at 300°C.

Likewise, there are other materials that are also used as fillers in polymer-based composites. Jang et al. studied the thermal degradation of clay/PA6 composites. They found that with only 2.5 wt% of clay the composites showed a degradation temperature 12 °C higher than the degradation temperature for the neat PA6. They obtained up to a 50% of weight loss for both, neat PA6 and composites, in a temperature range of 471-476 °C. The researchers found that one of the most significant evolved products during the degradation process is ϵ -caprolactam which has a boiling point of 271 °C. [57], [67] Therefore, since in the present study the temperatures that are used to process the CNTs/PA6 composites are higher than 271 °C, ϵ -caprolactam could be one of the major products formed after the thermal treatment. Some investigations have proved the presence of other products such as nitrile and unsaturated PA6 aliphatic chain ends. [57], [67]

Similarly, other fillers have been used to enhance the thermal properties of PA6 delaying its degradation under high temperatures. Li et al. studied the thermal behavior of aluminum hypophosphites (AlHP) and/or magnesium hypophosphites (MgHP)/PA6 composites. In order to understand the flame retardancy, study the thermal degradation of the composites was essential. The researchers found that neat PA6 only presents decomposition at 441 °C with a decomposition rate of 24.5 wt%/min. They found 5.8 wt% of char residue coming from the PA6 decomposition at 700 °C. With 24 wt% of AlHP the degradation temperature of the composites decreased until reaching 396 °C, but the decomposition rate resulted to be slower than the neat PA6, 13.7 wt%/min, with a 26 wt% of char residue at 700 °C. In the case of the composites containing 24 wt% of MgHP, the decomposition temperature was at 416 °C and the decomposition rate was 16.6 wt%/min. The researchers concluded that AlHP particles promote the PA6 degradation earlier than MgHP. They also compared the composites' degradation under both, air and nitrogen atmosphere. They found that the composites' decomposition process is more complex under air than under nitrogen. TGA results presented a two-steps degradation process for neat PA6 under air, at 427 and at 550 °C, and one-step process under nitrogen, similar to the case of the p-MWNT/PA6 composites previously explained (refer to mechanism from Figure 4. 10). For both type of composites, AlHP/PA6 and MgHP/PA6, the decomposition process was similar to the one under nitrogen atmosphere, meaning that was one-step process; however, the decomposition rate was very low for both. They attributed this phenomenon to the inhibiting effect of P-containing (phosphorous atoms), which is considered to be produced by the reaction P-O bond with oxygen, radicals on the radical degradation of PA6. [68]

CHAPTER 5. MECHANICAL PROPERTIES OF CARBON NANOTUBES/POLYAMIDE 6 COMPOSITES

Two mechanical properties were tested in CNT/PA6 composites fabricated in this study, hardness and modulus of elasticity. The hardness of each samples was tested at a microscale (in an order of magnitude between 1-100 μm), while the elastic modulus was tested at a macroscale (in an order of magnitude of millimeters). In this chapter will be discussed the results obtained from the Vickers Hardness test and the Dynamic Mechanical Analysis.

5.1. VICKERS HARDNESS

An average of at least ten indentations, each indentation was taken in the composites' cross-sectional area, were performed to obtain the Vickers Hardness (HV) values for each sample. Figure 5. 1 shows the HV (in MPa) values for the composites containing multi-walled carbon nanotubes. Here, three different MWCNTs concentrations from 45 wt% to 65 wt% are presented. All of them were processed with a 0.30 mm thick spacer and at 280 °C. For each batch of MWCNTs/PA6 composites, two different pressures were applied during the heat treatment, 5 MPa (see Figure 5. 1) and 10 MPa (see Figure 5. 2). For neat or pure PA6 (p-PA6), a HV value of 50.43 ± 1.74 MPa was obtained. The provider of PA6 reported a Hardness-Rockwell of M82. This is a special measurement scale for soft materials. In order to make a comparison, the Vickers Hardness was also measured for neat PA6. For the composites with an applied pressure of 5 MPa, the obtained HV values were 189.48 ± 31.67 , 122.54 ± 21.61 , and 100.87 ± 15.05 MPa for the compositions of 45, 55, and 65 wt%, respectively (see Figure 5. 1). It is shown that the composites with the lowest concentration (45 wt%) presents a higher HV value. A possible explanation for those low HV values in the composites with higher composition than 45 wt% can be that, after occurring PA6 degradation during the composites' fabrication, there may be not enough polymer to cover all the CNTs. However, it is clear that the addition of CNT improves the load carrying capacity of the PA6. According to Meng et al. the Vickers micro-hardness of PA6 also increased after adding 1.0 wt% of CNTs. Meng and collaborators reported HV values of 73.01 ± 0.45 MPa and 90.95 ± 0.62 MPa for p-PA6 and 1.0 wt% CNTs/PA6 composites, respectively. [69] According to Kuzumaki, CNTs help to improve a material hardness, because of their behavior as one-dimensional fine particles and because of its high modulus of elasticity. [70]

It is important to mention that, for each measurement to be valid under this test, the indentations had to be done in regions with extremely low (almost none) defect content. Since this is a micro-scale analysis, it was not difficult to find regions with no defects.

Moreover, Figure 5. 2 shows the HV values for the composites to which was applied a pressure of 10 MPa during the heat treatment. For the composites containing 45, 55, and 65 wt%, the obtained HV values were 227.66 ± 16.05 , 226.42 ± 28.35 , 95.92 ± 11.29 MPa, respectively. These results also show a higher HV value for the composites with low CNT concentration (45 wt%). Comparing the HV values for the composites where a pressure of 5 MPa was applied with those with an applied pressure of 10 MPa, it is seemed that the applied pressure during the heat treatment could also be an important factor that affects the material's hardness. A possible explanation can be that the pressure might be facilitating the wetting process of the CNT with the polymeric matrix during the heat treatment. Zhang et al. used 15 MPa to fabricate 1.0 wt% MWCNT/PA6 film composites and they obtained samples with a relative low number of defects and a higher hardness value compared with the neat PA6 (100 ± 0.002 MPa). [71]

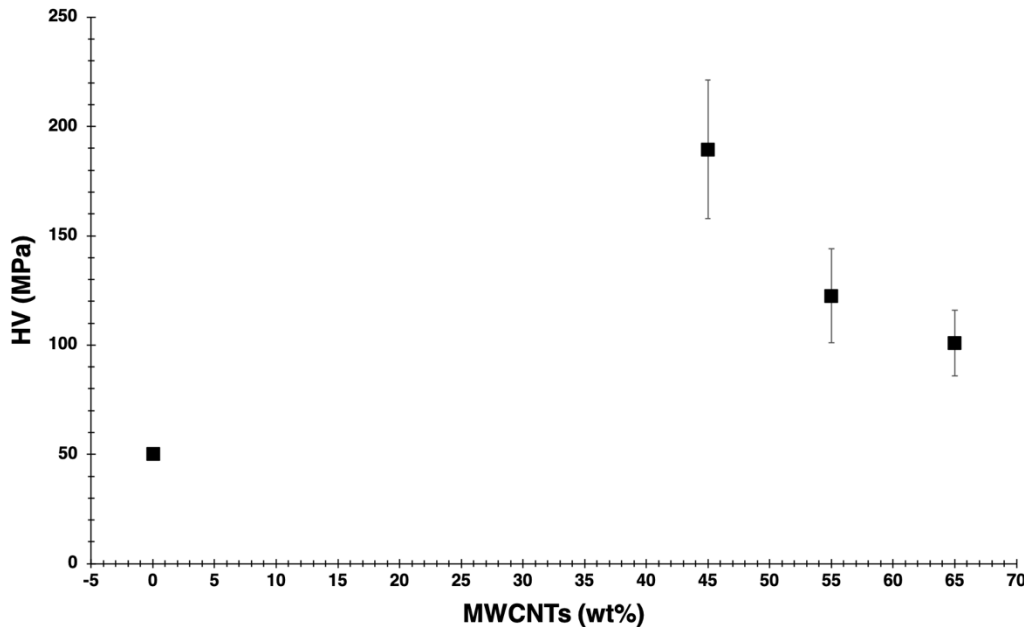


Figure 5. 1. Hardness test for MWCNT/PA6 composites with different CNT concentrations and processed with a 0.30 mm thick spacer, at 280 °C with an applied pressure of 5 MPa.

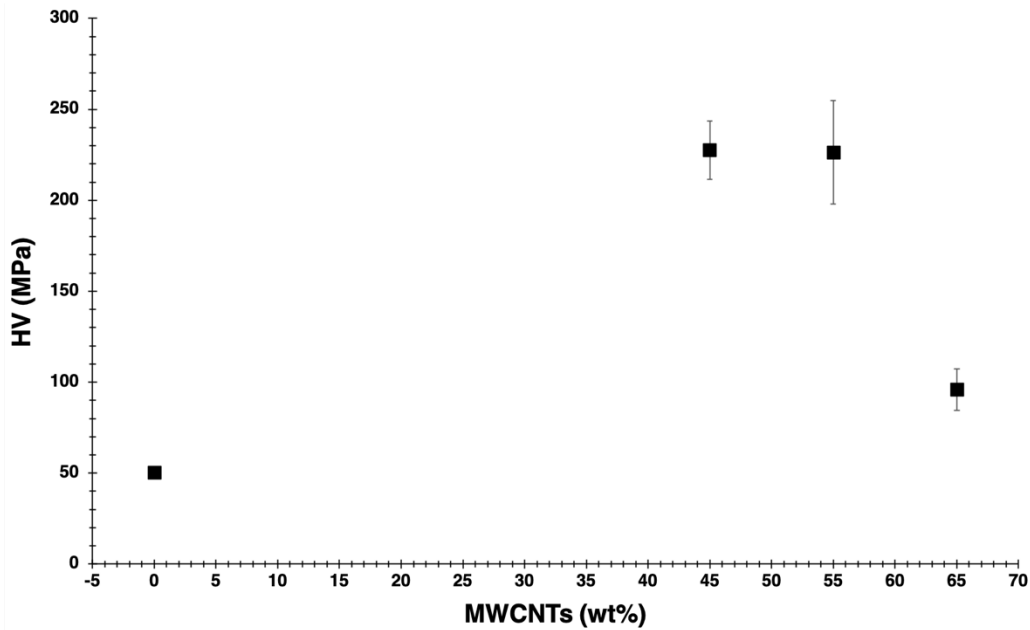


Figure 5. 2. Hardness test for MWCNT/PA6 composites with different CNT concentrations and processed with a 0.30 mm thick spacer, at 280 °C with an applied pressure of 10 MPa.

Figure 5. 3 shows the HV values for 55 wt% SWCNT/PA6 and 55 wt% MWCNT/PA6 composites. Both types of composites were processed with a 0.30 mm thick spacer, at 280 °C and with an applied pressure of 5 MPa. A HV value of 122.542 ± 21.61 MPa was obtained for the composites that had MWCNTs as fillers. On the other hand, for the composites containing SWCNTs, the HV value was of about 145.483 ± 61.22 MPa. A slightly difference in the HV values obtained for the composites with each type of fillers was observed. More experimental data will be required in order to reach stronger conclusions about the effect of the CNT type, if there is any, in the hardness of the composite.

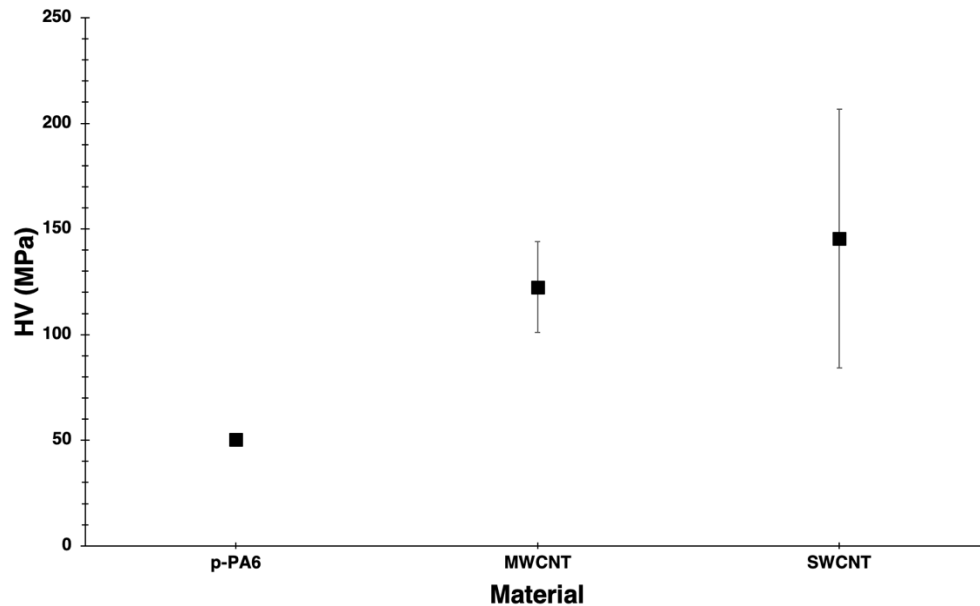


Figure 5. 3. Hardness test for 55 WT% CNTs/PA6 composites processed with a 0.30 mm thick spacer, at 280 °C, and with an applied pressure of 5 MPa.

5.2. ELASTIC MODULUS OF CARBON NANOTUBES/POLYAMIDE 6 COMPOSITES

Figure 5. 4 shows the stress versus strain curve of the composites containing 55 and 60 wt% of CNTs, green and red lines, respectively. These two types of composites were processed with an applied pressure of 5 MPa. In this curve, the behavior of a sample containing 65 wt% of CNTs and that were processed with an applied pressure of 10 MPa is presented (blue line). The samples with these compositions and processing parameters were the only ones that were able to test under this method. The rest of the samples presented a fragile behavior and they broke easily, making impossible to complete the dynamic analysis. However, a noticeable difference on the elastic modulus slope and in the rupture of the samples containing 65 wt% of CNTs and which were processed with 10 MPa, in comparison with the other presented composites, can be observed. Based on this difference, even though the compositions are slightly different, it can be inferred that the applied pressure plays an important role during the composites' fabrication and it can enhance their mechanical properties. As was mentioned before, applying a specific amount of pressure can contribute to the wrapping process of the CNTs by the polymer.

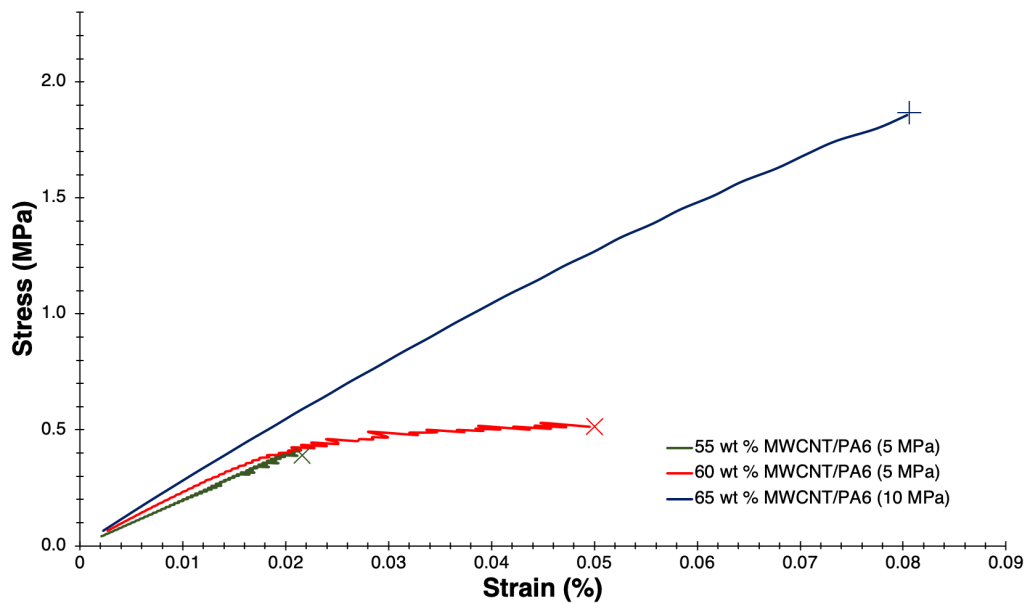


Figure 5. 4. Stress versus strain curve for CNT/PA6 composites.

Figure 5. 5 shows the relation between the modulus of elasticity, obtained from the dynamic mechanical analysis (DMA), with the CNT concentration (wt%) in the matrix. For composites with the following concentrations: 55, 60, 65 wt%, the obtained elastic modulus value is 19.68 ± 0.002 , 21.35 ± 0.004 , and 25.29 ± 0.012 MPa, respectively. The provider of the polyamide reported an elastic modulus range of 2600-3000 MPa. In this study, pure PA6 was treated with the same thermal process that was used to fabricate the composites. However, the processed pure PA6 sample resulted extremely brittle and performing a dynamic analysis was not possible. The behavior of the processed PA6 is very different from the non-processed PA6, because the polymer crystallizes during the heat treatment, and for this reason the polymer becomes brittle. The crystallinity percentage of the polyamide is something that we do not have clear in this study. Comparing the appearance of the processed PA6 sample with the one of the CNT/PA6 composites films, it could be said that the addition of CNTs can improve the elastic modulus of the treated PA6 and make it less brittle. Low elastic modulus values are reported in this research. One of the principal reasons of these low values is the huge number of defects that are found in the composites due to the PA6 degradation. Defects in the samples represent stress concentration and when a force is applied, they tend to break easily. The values obtained from both, hardness and tensile tests are very different. The principal reason of this difference is that the hardness test was carried at a micro-scale in those regions with almost no defects were found.

On the other hand, tensile tests were performed at a macroscale where all the defects were taken in consideration.

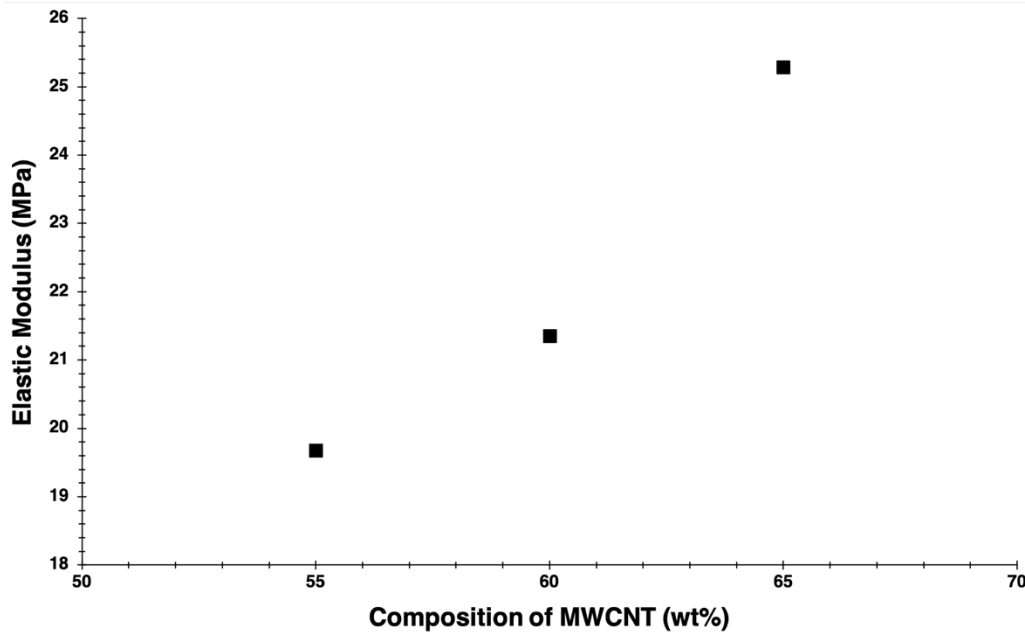


Figure 5. 5. Values of elastic modulus for MWNT/PA6 composites at different CNT concentrations.

Since the elastic modulus of non-functionalized CNT/PA6 composites is very low, many researchers have tried to modify the CNTs' surface in order to improve their interaction with PA6. Zhang et al. studied the mechanical properties of functionalized-MWCNTs/PA6 film composites prepared by melt-compound method. They reported an elastic modulus value of 852.4 MPa for composites containing only 1.0 wt% of MWCNTs. One of the reasons of this great improvement is the addition of carboxylic and hydroxyl groups on the CNT surface to enhance the interface interaction between the PA6 and the CNTs and to also obtain better CNT dispersion in the matrix. According to the authors, the PA6 becomes brittle after adding some amount of CNT. They observed that the sample broke at an elongation of 125% after adding 1.0 wt% of MWCNT, and the pure PA6 normally breaks above a 150% of elongation. [72] Furthermore, other researchers have performed a similar procedure to fabricate functionalized-MWCNTs/PA6 film composites by the melt-compounding method. Elastic modulus values from 1242 to 3556 MPa have been found for composites with a CNT concentration in the range of 0.0–2.0 wt%. [73], [74]

Moreover, Gao et al. reported functionalized-SWCNT/PA6 composite fibers with a concentration filler between 0.1-1.5 wt%. They found a proper CNT grafting with the PA6 due to the functionalization step. The researchers reported a modulus of elasticity of about 440 MPa, for the sample containing 1.5 wt% of SWCNTs, value which was slightly higher than the pure PA6 film (396 MPa). They suggest that the relative low elastic modulus is due to the small draw ratio of the fiber. The researchers found a decreasing in the break strain, the pure PA6 breaks at a strain of 418% and the fibers containing 1.5 wt % of SWCNTs break at 122%. According to the researchers, that decreasing in strain is an indicative of brittleness in the sample. [75] Other CNT/PA6 structures have been studied, besides CNT/PA6 film composites, Baji et al. reported elastic modulus and hardness values for CNT/PA6 fibers. For the fibers containing a CNT composition in the range of 0.0-7.5 wt %, they obtained elastic modulus values from ~ 1.0 to 2.5 GPa and hardness values between ~ 250 to 280 MPa. This was a proportional relation, meaning that at higher CNT content higher values of elastic modulus and hardness. [76]

Further on, composites using PA6 as matrix, with fillers different than CNTs, have been also studied. Handge et al. studied the mechanical properties of silicate nanotubes (from the halloysite mineral) and PA6 composites. They performed the mechanical tests at room temperature, which is below the PA6 T_g , and at 80 °C which is above of T_g . They obtained high elastic modulus values for the composites tested at room temperature and containing 30 wt% of halloysite (approximately 5000 MPa). According to the researchers, the elastic modulus of the composites tested at 80 °C is lower than the samples tested at room temperature, because the amorphous phase of PA6 is not in the glassy state and the composite behave more ductile. The authors also reported an increasing of brittleness in the composites containing halloysite concentrations above 10 wt%, which is similar to the behavior of the CNT/PA6 composites. [77]

CHAPTER 6. CONCLUSIONS AND FUTURE WORK

6.1. CONCLUSIONS

Both, SWCNT/ and MWCNT/polyamide 6 composites were fabricated using an innovating hot-pressing process where there was no need to use any kind of solvent. Pressure was applied during the material processing in order to minimize the number of defects in the samples. Non-functionalized and non-purified CNTs were used as fillers for each composite. Under the fabrication method presented in this study, CNT/PA6 composites with higher CNT concentration than ever reported were successfully obtained. SEM images taken from the cross-sectional area of the composites showed an effective CNTs wetting with the polymer, making a non-covalent interaction between the CNT surface and the PA6 chains. Defects in the samples were observed due to a poor dispersion of CNTs in the polymeric matrix. Lower number of defects in the samples that were processed with high pressure (10 MPa) were observed, in comparison to the composites that were processed with an applied pressure of 5 MPa. This demonstrates that the pressure has an effect on the CNTs dispersion in the matrix.

Additionally, polymer decomposition was detected from the thermal gravimetric analysis (TGA). This degradation can explain the several number of defects in the composites. It was found that under air atmosphere pure PA6 degradation occurs faster than under nitrogen atmosphere. In the case of CNT/PA6 composites, the degradation process is faster at 300 °C than at 280 °C. A possible explanation of this is that near to 300 °C, primary reactions in the PA6 chains, such as bonds breaking in some of the functional groups, might be occurring. Water storage in the PA6 chains might be a possible justification of the abrupt weight loss at the beginning of each TGA curve.

Furthermore, HV and elastic modulus values were obtained for the composites. An improvement in the composite's hardness and elastic modulus was found after the addition of CNTs. Higher HV values were obtained for the samples containing 45 wt% of CNTs. A high HV value (227.66 ± 16.05 MPa) was obtained for the samples containing 45 wt% of CNTs and that were processed with an applied pressure of 10 MPa, in comparison to the samples where a pressure of 5 MPa was applied (189.48 ± 31.67 MPa). No significant difference was found between the HV values of the samples containing SWCNTs and the ones containing MWCNTs.

In this study, composites with higher hardness values were obtained in comparison to the values reported in other studies and this could be due to the high concentrations of CNTs that were used (45-65 wt%). On the other hand, high elastic modulus values were obtained for the composites containing high concentrations of CNTs. For the composites containing 65 wt%, an elastic modulus of 25.29 ± 0.012 MPa was found. The elastic moduli values obtained in this experiment are lower than the ones reported in the literature, a possible explanation of this could be the elevated number of defects in the samples due to the possible PA6 degradation during the heat treatment. It is important to mention that the hardness and the tension tests were performed at a different scale. The HV values of the samples were measured at a microscale and their modulus of elasticity values were obtained from a DMA, which is performed in a macro-scale. As it is expected, the behavior of a material at a micro-scale differs from its behavior at a macro-scale. For this reason, more experimentation will be required, in order to make comparisons between these two mechanical properties in the composites.

After this study, a better understanding of the interaction between the CNTs and PA6 was obtained. There might be needed more experimentation to prove whether or not these composites are capable to substitute carbon fiber-based composites in the manufacturing of automotive and airplane parts. Carbon nanotubes/polymer composites is a relative new area of study and there are many things to know about it before implementing them.

6.2. FUTURE WORK

The conclusions obtained in this research make us to formulate new questions which might give a new huge pathway for future research in this field. Some of these questions are:

- Using purified CNTs in the fabrication process will help to improve the mechanical properties of the composites?
- What would happen if higher pressures are applied during the processing? Which is the maximum pressure that can be applied before to permanently deform the CNTs?
- What might happen if the composites are fabricated by this method, but under an argon or nitrogen atmosphere instead of under air atmosphere?
- Using a ceramic material (e.g. alumina) as spacer instead of a stainless-steel spacer during the fabrication step will help to stabilize the system absorbing heat and avoiding the polymer degradation?
- How the interaction of the CNTs would be with other thermoplastic polymers (e.g. polycarbonate)?

REFERENCES

- [1] L. Wood, "Global Composites Market 2012-2018 & 2022 - Market is Projected to Reach \$ 42 Billion," *Research and Markets Magazine*, 2018.
- [2] S. Mraz, "Carbon Fiber Composite Market to Hit \$31 Billion by 2024." 2018.
- [3] R. Mazumder, P. Sujatha Devi, D. Bhattacharya, P. Choudhury, A. Sen, and M. Raja, "Ferromagnetism in nanoscale BiFe O₃," *Appl. Phys. Lett.*, vol. 91, no. 6, pp. 91–94, 2007.
- [4] H. Margenau, "Van der Waals forces," *Rev. Mod Phys.*, vol. 11, no. 1, p. 1, 1939.
- [5] F. Dalmas *et al.*, "Multiwalled carbon nanotube/polymer nanocomposites: processing and properties," *J. Polym. Sci. Part B Polym. Phys.*, vol. 43, no. 10, pp. 1186–1197, 2005.
- [6] J. Kong, A. M. Cassell, and H. Dai, "Chemical vapor deposition of methane for single-walled carbon nanotubes," *Chem. Phys. Lett.*, vol. 292, no. 4–6, pp. 567–574, 1998.
- [7] D. Bhattacharyya, P. Maitrot, and S. Fakirov, "Polyamide 6 single polymer composites," *Express Polym. Lett.*, vol. 3, no. 8, pp. 525–532, 2009.
- [8] L. Chen *et al.*, "Fabrication and characterization of polycarbonate/carbon nanotubes composites," *Compos. Part A Appl. Sci. Manuf.*, vol. 37, no. 9, pp. 1485–1489, 2006.
- [9] F. Y. Castillo *et al.*, "Electrical, mechanical, and glass transition behavior of polycarbonate-based nanocomposites with different multi-walled carbon nanotubes," *Polymer (Guildf)*, vol. 52, no. 17, pp. 3835–3845, 2011.
- [10] O. Breuer and U. Sundararaj, "Big returns from small fibers: A review of polymer/carbon nanotube composites," *Polym. Compos.*, vol. 25, no. 6, pp. 630–645, 2004.
- [11] S. Arun and S. Kanagaraj, "Performance enhancement of epoxy based sandwich composites using multiwalled carbon nanotubes for the application of sockets in trans-femoral amputees," *J. Mech. Behav. Biomed. Mater.*, vol. 59, pp. 1–10, 2016.
- [12] N. Mahmood, M. Islam, A. Hameed, and S. Saeed, "Polyamide 6/multiwalled carbon

- nanotubes nanocomposites with modified morphology and thermal properties,” *Polymers (Basel)*., vol. 5, no. 4, pp. 1380–1391, 2013.
- [13] S. Pande, A. Chaudhary, D. Patel, B. P. Singh, and R. B. Mathur, “Mechanical and electrical properties of multiwall carbon nanotube/polycarbonate composites for electrostatic discharge and electromagnetic interference shielding applications,” *RSC Adv.*, vol. 4, p. 13839, 2014.
- [14] G. Palardy, D. Trudel-Boucher, and P. Hubert, “Investigation of a postprocessing method to tailor the mechanical properties of carbon nanotube/polyamide fibers,” *J. Appl. Polym. Sci.*, vol. 130, no. 6, pp. 4375–4382, 2013.
- [15] E. Asedegbega-Nieto, M. Pérez-Cadenas, J. Carter, J. a Anderson, and A. Guerrero-Ruiz, “Preparation and surface functionalization of MWCNTs: study of the composite materials produced by the interaction with an iron phthalocyanine complex.,” *Nanoscale Res. Lett.*, vol. 6, no. 1, p. 353, 2011.
- [16] P. Jindal, M. Goyal, and N. Kumar, “Mechanical characterization of multiwalled carbon nanotubes-polycarbonate composites,” *Mater. Des.*, vol. 54, pp. 864–868, 2014.
- [17] S. Sharma, R. Chandra, P. Kumar, and N. Kumar, “Thermo-mechanical characterization of multi-walled carbon nanotube reinforced polycarbonate composites: A molecular dynamics approach,” *Comptes Rendus - Mec.*, vol. 343, no. 5–6, pp. 371–396, 2015.
- [18] V. Tishkova *et al.*, “Uniform dispersion of nanotubes in thermoplastic polymer through thermal annealing,” *Carbon N. Y.*, vol. 53, pp. 399–402, 2013.
- [19] T. Morishita, Y. Katagiri, T. Matsunaga, Y. Muraoka, and K. Fukumori, “Design and fabrication of morphologically controlled carbon nanotube/polyamide-6-based composites as electrically insulating materials having enhanced thermal conductivity and elastic modulus,” *Compos. Sci. Technol.*, vol. 142, pp. 41–49, Apr. 2017.
- [20] D. R. . Askeland, F. . Pradeep, and W. J. Wright, *The science and engineering of materials*. 2010.

- [21] A. Kumar and K. Gupta, Rakesh, *Fundamentals of Polymer Engineering*, vol. 80, no. 1. 2005.
- [22] J. P. . Schaffer, A. Saxena, S. D. . Antolovich, J. T. H. . Sanders, and S. B. Warner, *The Science and Design of Engineering Materials*. .
- [23] D. M. . Guldi and N. Martín, *Carbon Nanotubes and Related Structures*. 1999.
- [24] M. Rahmandoust and M. R. Ayatollahi, *Characterization of Carbon Nanotube Based Composites under Consideration of Defects*, vol. 39. 2016.
- [25] C. W. S. To, “Bending and shear moduli of single-walled carbon nanotubes,” *Finite Elem. Anal. Des.*, vol. 42, no. 5, pp. 404–413, 2006.
- [26] K. I. Tserpes and P. Papanikos, “Finite element modeling of single-walled carbon nanotubes,” *Compos. Part B Eng.*, vol. 36, no. 5, pp. 468–477, 2005.
- [27] C. Li and T. W. Chou, “A structural mechanics approach for the analysis of carbon nanotubes,” *Int. J. Solids Struct.*, vol. 40, no. 10, pp. 2487–2499, 2003.
- [28] M. S. Dresselhaus, G. Dresselhaus, and R. Saito, “Physics of carbon nanotubes,” *Carbon N. Y.*, vol. 33, no. 7, pp. 883–891, 1995.
- [29] T. Natsuki, K. Tantrakarn, and M. Endo, “Prediction of elastic properties for single-walled carbon nanotubes,” *Carbon N. Y.*, vol. 42, no. 1, pp. 39–45, 2004.
- [30] S. Iijima and T. Ichihashi, “Single-shell carbon nanotubes of 1-nm diameter,” *Nature*, vol. 363, no. 6430, pp. 603–605, 1993.
- [31] A. L. Kalamkarov, A. V. Georgiades, S. K. Rokkam, V. P. Veedu, and M. N. Ghasemi-Nejhad, “Analytical and numerical techniques to predict carbon nanotubes properties,” *Int. J. Solids Struct.*, vol. 43, no. 22–23, pp. 6832–6854, 2006.
- [32] G. Ghadyani and M. Rahmandoust, “Computational Nanomechanics Investigation Techniques,” 2016.

- [33] M. M. A. Rafique and J. Iqbal, "Production of Carbon Nanotubes by Different Routes — A Review," *J. Encapsulation Adsorpt. Sci.*, vol. 1, no. June, pp. 29–34, 2011.
- [34] W. Z. Li *et al.*, "Large-scale synthesis of aligned carbon nanotubes," *Sci. (Washington, D. C.) F. Full J. TitleScience (Washington, D. C.)*, vol. 274, no. 5293, pp. 1701–1703, 1996.
- [35] M. Wilson, K. Kannangara, G. Smith, M. Simmons, and B. Raguse, *NANOTECHNOLOGY Basic Science and Emerging Technologies*. 2002.
- [36] C. Wei, D. Srivastava, and K. Cho, "Thermal Expansion and Diffusion Coefficients of Carbon Nanotube-Polymer Composites," *Nano Lett.*, vol. 2, no. 6, pp. 647–650, 2002.
- [37] C. P. Deck and K. Vecchio, "Growth mechanism of vapor phase CVD-grown multi-walled carbon nanotubes," *Carbon N. Y.*, vol. 43, no. 12, pp. 2608–2617, 2005.
- [38] A. Ghavamian and A. Öchsner, "Numerical modeling of eigenmodes and eigenfrequencies of single- and multi-walled carbon nanotubes under the influence of atomic defects," *Comput. Mater. Sci.*, vol. 72, pp. 42–48, 2013.
- [39] J. William D. Callister and David G. Rethwisch, *Materials science and engineering: An introduction*. 2010.
- [40] C. H. Chen and C. H. Cheng, "Effective elastic moduli of misoriented short-fiber composites," *Int. J. Solids Struct.*, vol. 33, no. 17, pp. 2519–2539, 1996.
- [41] W. Haitao and Y. A. O. Zhenhan, "Large Scale Analysis of Mechanical Properties in 3-D Fiber-Reinforced Composites Using a New Fast Multipole Boundary Element Method * for an Elastic Domain Containing," vol. 12, no. 5, pp. 554–561, 2007.
- [42] K. K. Chawla, *Composite Materials Science and Engineering*, vol. 72. 2017.
- [43] M. Richard, M. Vennett Stanley, P. Wolf, P. Albert, and Levitt, "Multiple Necking of Tungsten Fibers in a Brass-Tungsten Composite," *Metall. Trans.*, vol. 1, no. June, p. 1569, 1970.
- [44] C. Schoene and E. Scala, "Multiple necking phenomena in metal composites," *Metall.*

Trans., vol. 1, no. 12, pp. 3466–3469, 1970.

- [45] P. M. Ajayan, “Nanotubes from Carbon,” *Chem. Rev.*, vol. 99, no. 7, pp. 1787–1800, 1999.
- [46] C. Goze, L. Vaccarini, L. Henrard, P. Bernier, E. Hernandez, and A. Rubio, “Elastic and mechanical properties of carbon nanotubes,” *Synth. Met.*, vol. 103, no. 1–3, pp. 2500–2501, 1999.
- [47] M. S. Dresselhaus and P. Avouris, “Introduction to Carbon Materials Research,” *Carbon Nanotub.*, vol. 9, pp. 1–9, 2001.
- [48] X. L. Xie, Y. W. Mai, and X. P. Zhou, “Dispersion and alignment of carbon nanotubes in polymer matrix: A review,” *Mater. Sci. Eng. R Reports*, vol. 49, no. 4, pp. 89–112, 2005.
- [49] M. Guerrero Fernández and C. Marín Martín, “Experimental Benchmarks for Mechanical Properties of Highly-loaded Carbon Nanotube- Reinforced Polyether Ether Ketone,” 2018.
- [50] C. Zhao *et al.*, “Synthesis and characterization of multi-walled carbon nanotubes reinforced polyamide 6 via in situ polymerization,” *Polymer (Guildf)*., vol. 46, no. 14, pp. 5125–5132, 2005.
- [51] A. C. Brosse, S. Tencé-Girault, P. M. Piccione, and L. Leibler, “Effect of multi-walled carbon nanotubes on the lamellae morphology of polyamide-6,” *Polymer (Guildf)*., vol. 49, no. 21, pp. 4680–4686, 2008.
- [52] R. Andrews, D. Jacques, M. Minot, and T. Rantell, “Fabrication of Carbon Multiwall Nanotube / Polymer Composites by Shear Mixing NA,” *Macromol. Mater. Eng.*, vol. 287, no. 6, pp. 395–403, 2002.
- [53] E. T. Thostenson and T.-W. Chou, “Aligned multi-walled carbon nanotube-reinforced composites: processing and mechanical characterization,” *J. Phys. D. Appl. Phys.*, vol. 35, no. 16, pp. L77–L80, 2002.
- [54] J. Li, L. Tong, Z. Fang, A. Gu, and Z. Xu, “Thermal degradation behavior of multi-walled carbon nanotubes / polyamide 6 composites,” vol. 91, pp. 2046–2052, 2006.

- [55] M. Henriksson and L. A. Berglund, "Structure and Properties of Cellulose Nanocomposites Films Containing Melamine Formaldehyde," *Appl. Polym. Sci.*, vol. 106, pp. 2817–2824, 2007.
- [56] S. Pegel, P. Pötschke, G. Petzold, I. Alig, S. M. Dudkin, and D. Lellinger, "Dispersion, agglomeration, and network formation of multiwalled carbon nanotubes in polycarbonate melts," *Polymer (Guildf.)*, vol. 49, no. 4, pp. 974–984, 2008.
- [57] S. V Levchik, E. D. Weil, and M. Lewin, "Thermal decomposition of aliphatic nylons," *Polym. Int.*, vol. 48, no. 7, pp. 532–557, 1999.
- [58] B. Lánská, D. Doskočilová, L. Matisová-Rychlá, R. Puffr, and J. Rychlý, "Thermooxidation of lactam-based polyamides with amino end-groups. Thermooxidation of hexano-6-lactam and decomposition of 6-hydroperoxyhexano-6-lactam in the presence of primary amines," *Polym. Degrad. Stab.*, vol. 63, no. 3, pp. 469–479, 1999.
- [59] J. Pagacz *et al.*, "Thermal decomposition studies of bio-resourced polyamides by thermogravimetry and evolved gas analysis," *Thermochim. Acta*, vol. 612, pp. 40–48, 2015.
- [60] S. V. Levchik, I. Balabanovich, G. Caminob, and L. Costab, "Mechanistic study of combustion performance and thermal decomposition behaviour of nylon 6 with added halogen free fire retardants," *Polym. Degrad. Stab.*, vol. 54, no. 2–3, pp. 217–222, 1996.
- [61] A. Ballistreri, D. Garozzo, M. Giuffrida, G. Impallomeni, and G. Montaudo, "Primary Thermal Decomposition Processes in Aliphatic Polyamides," *Polym. Degrad. Stab.*, vol. 23, pp. 25–41, 1988.
- [62] B. Zhao, L. Chen, J. Long, H. Chen, and Y. Wang, "Aluminum Hypophosphite versus Alkyl-Substituted Phosphinate in Polyamide 6 : Flame Retardance , Thermal Degradation , and Pyrolysis Behavior," *Ind. Eng. Chem. Res.*, vol. 52, pp. 2875–2886, 2013.
- [63] S. Smith, "The re-equilibration of polycapraamide," *J. Polym. Sci.*, vol. 30, no. 121, pp. 459–478, 2003.
- [64] C. Guaita, "HPLC Analysis of cyclo-oligoamides 6 and 66 ," *Makromol. Chemie*, vol. 185,

- no. 3, pp. 459–465, 1984.
- [65] H. K. Reimschuessel and G. J. Dege, “Polyamides: Decarboxylation and desamination in nylon 6 equilibrium polymer,” *J. Polym. Sci. Part A-1 Polym. Chem.*, vol. 8, no. 11, pp. 3265–3283, 2003.
 - [66] A. A. Hanna, “Thermal and dielectric properties of nylon 6,” *Thermochim. Acta*, vol. 76, no. 1–2, pp. 97–103, 1984.
 - [67] B. N. Jang and C. A. Wilkie, “The effect of clay on the thermal degradation of polyamide 6 in polyamide 6 / clay nanocomposites,” vol. 46, pp. 3264–3274, 2005.
 - [68] Q. Li, B. Li, S. Zhang, and M. Lin, “Investigation on Effects of Aluminum and Magnesium Hypophosphites on Flame Retardancy and Thermal Degradation of Polyamide 6,” 2012.
 - [69] H. Meng, G. X. Sui, G. Y. Xie, and R. Yang, “Friction and wear behavior of carbon nanotubes reinforced polyamide 6 composites under dry sliding and water lubricated condition,” *Compos. Sci. Technol.*, vol. 69, no. 5, pp. 606–611, 2009.
 - [70] T. Kuzumaki, O. Ujiie, H. Ichinose, and K. Ito, “Mechanical Characteristics and Preparation of Carbon Nanotube Fiber-Reinforced Ti Composite,” *Adv. Eng. Mater.*, vol. 2, no. 7, pp. 416–418, 2000.
 - [71] W. De Zhang, L. Shen, I. Y. Phang, and T. Liu, “Carbon nanotubes reinforced nylon-6 composite prepared by simple melt-compounding,” *Macromolecules*, vol. 37, no. 2, pp. 256–259, 2004.
 - [72] W. De Zhang, L. Shen, and I. Y. Phang, “Carbon Nanotubes Reinforced Nylon-6 Composite Prepared by Simple Melt-Compounding,” pp. 256–259, 2004.
 - [73] T. Liu, I. Y. Phang, L. Shen, S. Y. Chow, and W. De Zhang, “Morphology and mechanical properties of multiwalled carbon nanotubes reinforced nylon-6 composites,” *Macromolecules*, vol. 37, no. 19, pp. 7214–7222, 2004.
 - [74] G. X. Chen, H. S. Kim, B. H. Park, and J. S. Yoon, “Multi-walled carbon nanotubes

- reinforced nylon 6 composites,” *Polymer (Guildf)*., vol. 47, no. 13, pp. 4760–4767, 2006.
- [75] J. Gao, M. E. Itkis, A. Yu, E. Bekyarova, B. Zhao, and R. C. Haddon, “Continuous spinning of a single-walled carbon nanotube– nylon composite fiber,” *J. Am. Chem. Soc.*, vol. 127, no. 11, pp. 3847–3854, 2005.
- [76] A. Baji, Y. W. Mai, S. C. Wong, M. Abtahi, and X. Du, “Mechanical behavior of self-assembled carbon nanotube reinforced nylon 6,6 fibers,” *Compos. Sci. Technol.*, vol. 70, no. 9, pp. 1401–1409, 2010.
- [77] U. A. Handge, K. Hedicke-Höchstötter, and V. Altstädt, “Composites of polyamide 6 and silicate nanotubes of the mineral halloysite: Influence of molecular weight on thermal, mechanical and rheological properties,” *Polymer (Guildf)*., vol. 51, no. 12, pp. 2690–2699, 2010.